



LEEDS
BECKETT
UNIVERSITY

Citation:

Parker, J and Fletcher, M and Thomas, F (2024) Characteristics of air temperature and thermal comfort in the grey and green spaces of an urban heat island. *Sustainable Environment*, 10 (1). pp. 1-21. ISSN 2765-8511 DOI: <https://doi.org/10.1080/27658511.2024.2424069>

Link to Leeds Beckett Repository record:

<https://eprints.leedsbeckett.ac.uk/id/eprint/11495/>

Document Version:

Article (Published Version)

Creative Commons: Attribution 4.0

© 2024 The Author(s)

The aim of the Leeds Beckett Repository is to provide open access to our research, as required by funder policies and permitted by publishers and copyright law.

The Leeds Beckett repository holds a wide range of publications, each of which has been checked for copyright and the relevant embargo period has been applied by the Research Services team.

We operate on a standard take-down policy. If you are the author or publisher of an output and you would like it removed from the repository, please [contact us](#) and we will investigate on a case-by-case basis.

Each thesis in the repository has been cleared where necessary by the author for third party copyright. If you would like a thesis to be removed from the repository or believe there is an issue with copyright, please contact us on openaccess@leedsbeckett.ac.uk and we will investigate on a case-by-case basis.



Sustainable Environment

An international journal of environmental health and sustainability

ISSN: (Print) (Online) Journal homepage: www.tandfonline.com/journals/oaes21

Characteristics of air temperature and thermal comfort in the grey and green spaces of an urban heat island

James Parker, Martin Fletcher & Felix Thomas

To cite this article: James Parker, Martin Fletcher & Felix Thomas (2024) Characteristics of air temperature and thermal comfort in the grey and green spaces of an urban heat island, Sustainable Environment, 10:1, 2424069, DOI: [10.1080/27658511.2024.2424069](https://doi.org/10.1080/27658511.2024.2424069)

To link to this article: <https://doi.org/10.1080/27658511.2024.2424069>



© 2024 The Author(s). Published by Informa UK Limited, trading as Taylor & Francis Group.



Published online: 07 Nov 2024.



Submit your article to this journal [↗](#)



Article views: 17



View related articles [↗](#)

Characteristics of air temperature and thermal comfort in the grey and green spaces of an urban heat island

James Parker , Martin Fletcher and Felix Thomas

School of the Built Environment, Engineering and Computing, Leeds Sustainability Institute, Leeds Beckett University, Leeds, UK

ABSTRACT

Urban green spaces are acknowledged as a vital component in a healthy city, providing a wealth of benefits. Urban green infrastructure (UGI) can help to moderate the intensity of the Urban Heat Island (UHI), there is however a lack of high temporal and spatial ground-level data that quantifies the impact of UGI on air temperature and human comfort within UHI areas, and particularly for cities in temperate marine climates, which are not comprehensively understood. This paper therefore uses data from a high-resolution monitoring campaign in the UK city of Leeds to describe the diurnal characteristics of air temperature in grey and green spaces between May and August 2021. Average UHI intensity during this period was 0.9 °K, with a summer maximum of 3.1 °K occurring in late evening. Although there is variation across the monitoring sites, green space was on average 0.7 °K cooler than the grey spaces during the summer months, and up to 2.6 °K cooler on some of the hottest days. Air temperature in urban woods was up to 4.0 °K cooler on the hottest days. These measured data demonstrate the influence of UGI on air temperature in UHI areas, and quantify the impact of different types of UGI, identifying the UGI types that are most effective at regulating higher summertime air temperature. Results presented here provide valuable quantitative data that can support the protection and expansion of urban green space as part of policy development and urban planning in practice.

ARTICLE HISTORY

Received 26 July 2024
Accepted 28 October 2024

KEYWORDS



Air temperature; microclimate; thermal comfort; urban green infrastructure; urban heat island

1. Introduction

Urban areas often experience higher temperature than the surrounding rural areas, a phenomenon described as the Urban Heat Island (UHI) (Akbari & Kolokotsa, 2016; Oke, 1976; Taha, 1997; Yamashita & Sekine, 1990). Human activities such as changes in land use and conditioning buildings have led to UHIs being observed throughout the world. The UHI effect has been recognised since the middle of the 20th century (Oke, 1976) and recent decades have seen a continual increase in UHI focused research, driven by the availability of remote sensing data, the wider deployment of maturing sensor technologies, growth in urban populations and the individual nature of each city's heat island (Mirzaei & Haghighat, 2010; Stewart, 2011). Hotter weather in Subtropical, Mediterranean and Arid climatic regions can lead to more extreme UHI intensity (UHII) (Akbari & Kolokotsa, 2016; Q. Huang & Lu, 2018; Stewart, 2011). However, UHI effects are also evident in cooler Maritime climates like that found in the UK, and climate change is expected to increase the intensity of heatwaves and the UHI in the future (Demanele et al., 2012; Levermore et al., 2015;

Oikonomou et al., 2012; Skelhorn et al., 2016; Taylor et al., 2017). The UHII in the city of Leeds during the period 7 May to 25 August 2021 is characterised in the first part of this paper, using measured near-ground air temperature data from a network of 57 sensors installed throughout the city; the Leeds UHI during the summer heatwave of 2013 has been quantified in previous work (Parker, 2021).

Installation and administrative requirements related to this size of sensor network in public urban spaces are non-trivial, and it is the authors' long-term professional working relationship with Leeds City Council that facilitated the deployment of this sensor network. Data from the network is shared with the City Council and will be used in future projects. It was the approval for the overall sensor network installations that led to the opportunity to study conditions in Leeds specifically. This work also uses third-party data from the ERA5 Copernicus Climate Data Store as a cross-reference with the local observations (Hersbach et al., 2023). Diurnal patterns of the UHII during this period are presented in the results, and the significance of the reference sites used to calculate the UHII is evaluated.

CONTACT James Parker  j.m.parker@leedsbeckett.ac.uk  School of the Built Environment, Engineering and Computing, Leeds Sustainability Institute, Leeds Beckett University, Churchwood House, Headingley Campus, Leeds LS6 3QJ, UK

© 2024 The Author(s). Published by Informa UK Limited, trading as Taylor & Francis Group.

This is an Open Access article distributed under the terms of the Creative Commons Attribution License (<http://creativecommons.org/licenses/by/4.0/>), which permits unrestricted use, distribution, and reproduction in any medium, provided the original work is properly cited. The terms on which this article has been published allow the posting of the Accepted Manuscript in a repository by the author(s) or with their consent.

The UHII conditions of smaller cities in Maritime climates are not as well understood in the existing literature, and access to high temporal and spatial resolution observations is lacking in these areas. Increased understanding of UHIs had led to exploration of potential mitigation methods (Aflaki et al., 2017; Akbari & Kolokotsa, 2016; Aleksandrowicz et al., 2017). Measures that can help to mitigate the UHII include the orientation of buildings to sun and wind, reflective coatings for buildings and land-cover (pavements and roads), and bodies of water and green infrastructure (Aleksandrowicz et al., 2017). The most commonly studied mitigation method is the use of urban green infrastructure (UGI) as the shade and evapotranspiration effects from trees, ground vegetation (parks and gardens for example), green roofs and green facades can all help to reduce urban air temperature (Aflaki et al., 2017; Akbari & Kolokotsa, 2016; Aleksandrowicz et al., 2017; Doick et al., 2014; Norton et al., 2015; Vaz Monteiro et al., 2016).

Measured data from the sensor network are used in the second part of this paper to characterise the variance between grey and green spaces. As noted above, there is currently a lack of high spatial and temporal resolution data collected at ground-level that quantifies these conditions. Diurnal patterns of the temperature differences are described, along with the context of the city's topography. These data are also used to compare thermal comfort in grey and green spaces using the Universal Thermal Climate Index (UTCI) metric (Blazejczyk et al., 2013). The UTCI has not previously been used to understand thermal comfort in this range of UGI categories, and in this type of urban climate. Ultimately, the aim of this work is to collate high-resolution data that quantifies the impact of UGI in UHI areas and provides a robust evidence base, that can in turn, help to inform policy development and urban planning practices; ultimately, this can support the retention of existing UGIs and incentivise the addition of new UGI areas.

2. Literature review

2.1. Urban heat island intensity

An Urban Heat Island (UHI) describes the relative warmer conditions found in built up areas when compared with the rural surroundings (Levermore et al., 2015; Oke, 1976). Higher urban air temperature and surface temperature are both associated with the UHI effect (Stewart, 2011). Study of the UHI can be divided into three categories, the canopy UHI (using ground level measurements), the boundary level UHI and the land surface UHI (Azevedo et al., 2016); this paper focuses on the canopy UHI using ground level air temperature measurements. Remote sensing data

from satellites can be used to quantify UHI effects on surface temperature for urban areas but inferring local air temperature from these data is a non-trivial exercise (Cui et al., 2017; Kawashima et al., 2000; Mahdavi et al., 2016). Inherently, satellites only provide data for specific short periods of time as they pass over parts of the Earth during their orbit, therefore near-ground measurements are the most effective means of characterising UHI effects on air temperature at a high temporal resolution (Mahdavi et al., 2016). As the focus of this paper is to explore the impact of UGI on air temperature and human comfort within a UHI area, the UHI values included in this section describe air temperature measurements within the urban canopy. More extreme effects of the UHI have been shown to be greatest during nocturnal hours, therefore ground level measurements play an important role in understanding diurnal patterns; daytime air and surface temperature can often be similar in UHI areas, whereas air temperature during the night can be significantly higher (Kamarianakis et al., 2017; Levermore & Parkinson, 2019; Levermore et al., 2015; Oke, 1982; Zhang et al., 2005). Higher night-time air temperature can exacerbate overheating and reduce the efficiency of mechanical cooling (Dobrovolný & Krahula, 2015; Giridharan et al., 2005; Kawashima et al., 2000; P. Zhang et al., 2010). Serious health conditions such as heat stress, heat rash and cramps, heat exhaustion, heat stroke, aggravation of cardiovascular disease, and, in the most seriously circumstances, premature death, have all been linked to the hotter conditions found in UHIs (Grimmond, 2007; Jenkins et al., 2014; Li et al., 2013; Mavrogianni et al., 2011; O'Lenick et al., 2019; Wu et al., 2014).

An average UHI intensity of between 1 °K and 3 °K has been estimated for large cities across the globe, but values differ from city to city as a range of local factors can influence how the UHI manifests (Guattari et al., 2018). Meteorological features such as wind speed and direction and cloud cover influence the UHI directly (Bernard et al., 2017; Oke, 1982) as do changes in landcover, with low albedo manmade materials and increased thermal mass leading to less heat being reflected and more heat being stored in the city as a whole (Mohajerani et al., 2017; Oke, 1982). In European cities, a mean UHI intensity of approximately 2.5 °K has been recorded, with summer peak intensities being much higher during nocturnal hours, measured data showing this can reach 8 °K in Barcelona and 16 °K in Athens (Santamouris, 2007). Similar peaks have been recorded in China and the USA, with nocturnal peaks of 8 °K and 5 °K recorded in Beijing and New York respectively (Cui et al., 2017; Gaffin et al., 2008). The daytime UHI in New York study has been shown to often be much lower and this

has been reflected by observations in the UK, where the UHI is principally a nocturnal issue (Kolokotroni et al., 2012; Levermore & Parkinson, 2019; Levermore et al., 2015; Taylor et al., 2017). An average daily UHI of 2 °K has been measured in London, however, night-time peaks in UK cities can be significantly higher, peak summertime values of 8 °K have been recorded in London and Manchester, and a peak value of over 7 °K has been observed in Birmingham (Azevedo et al., 2016; Levermore & Parkinson, 2016; Levermore et al., 2015; Tomlinson et al., 2013).

Whilst the focus of this work is on ground-level air temperature conditions, land surface temperature has been widely used to quantify the surface temperature UHI, with remote sensing data now being readily available (Kamarianakis et al., 2017; Zhang et al., 2005; Zhou et al., 2014); the density and physical layout of cities are strongly linked with high UHI conditions. Traditionally, landscape indicators have been used to characterise the spatial pattern of land use, but recent work has identified morphological spatial pattern analysis (MSPA) as a more effective means of characterising the morphology of urban areas in the context of UHI conditions, and the potential for green space to mitigate these effects (Lin et al., 2024). This study demonstrated that the quantity, compactness and spatial complexity of urban areas were highly related to increased land surface temperature, and that improving the quality of blue and green infrastructure and that these should be as 'orderly as possible' to most effectively mitigate against high levels of urban heat (J. Lin et al., 2024). Ideally, in the long-term, this would mean reducing the proportion of built up area through careful urban planning, if possible, as the density and area of built up areas is strongly connected to high land surface temperatures, a significant contributor to the overall UHI.

2.2. Green infrastructure mitigation of urban heat island intensity

Green infrastructure, including parks, trees, green roofs, and green façades can all help to reduce UHI, along with other measures such as reflective coatings (Akbari & Kolokotsa, 2016; Aleksandrowicz et al., 2017). It is important to note that different heat mitigation strategies introduced to urban areas (for example green roofs, reflective surfaces and street trees) can cause indirect impacts. These can be positive, for instance, green roofs can reduce urban heat and also reduce cooling energy demand of buildings (Huang et al., 2023). Hedges in urban streets can add to the evapotranspiration within their microclimate, whilst promoting biodiversity

(Sauerbrei et al., 2017) and mitigating against air pollution through their dense form and low height (Kumar et al., 2022). However, some heat mitigation strategies might have negative impacts. For example, reflective pavements can cause glare or visual discomfort for pedestrians and increase the heat load on human beings are subjected to (Erell et al., 2014). Successful design of heat mitigation strategies therefore requires careful consideration of the local environment.

In drier climates reflective pavements can have significant impacts as well; a study in Greece has shown that 4500 m² of cool pavements within a park in Athens helped reduced surface and air temperatures by 12 °K and 1.9 °K respectively (Santamouris et al., 2012). Most research suggests that UGI helps to reduce local air temperature but the complex biological processes of plants can sometimes lead to warming during different parts of the day and in different seasons (Meili et al., 2021). Meili et al cite global examples of daytime cooling effects from trees being between 0.5 °K and 3.5 °K, which is reduced to between 0.3 °K and 0.5 °K overnight, but also cite examples of warming during nocturnal hours of up to 0.6 °K (Meili et al., 2021). Warming effects from trees during springtime and summertime daylight hours have been observed between 0.2 °K and a maximum of 0.7 °K, partly due to the evapotranspiration process and latent heat transfer (Meili et al., 2021).

Research based upon both measurement and modelling has been carried out to help quantify the extent to which UGI can help mitigate the UHI. Measurement of grey and green space at a high resolution can be resource intensive, therefore physical modelling approaches provide a useful means to understand the mitigation potential of green space. Physical law-driven models can theoretically quantify the influence of green infrastructure on microclimates, these have been used to predict that green roofs can reduce discrete local air temperature by between 0.4 °K and 1.7 °K, and green façades by 1.6 in tropical climates; modelled data also predicts peak reductions as high as 4 °K for green roofs alone (Chandramathy & Kitchley, 2018; Herath et al., 2018a, 2018b; Ng et al., 2012; Santamouris, 2014). Modelled results agree with measured data, monitored green roofs have been shown to reduce air temperature by 0.3 °K and 2.4 °K in tropical climates (Konasova, 2017; Sun et al., 2012). A UK study measured an average local reduction from green roofs of 1.1 °K (Speak et al., 2013).

2.3. Mitigation of urban heat island intensity from green spaces

Larger UGI areas, including trees, small parks and larger parks containing a mixture of UGIs, can be modelled to

simulate wider impacts. Small groups of trees have been modelled with results indicating a reduction of air temperature by between 0.8 °K and 1.5 °K, similar models suggest parks can reduce air temperature by between 1 °K and 1.8 °K (Herath et al., 2018a; Ng et al., 2012). A data-driven model that combines remote sensing and ground level observations estimates UGI in European cities cools them by an average of 1.07 °K, and up to 2.9 °K in hotter climates (Marando et al., 2022). Some smaller scale studies comparing localised air temperature within a microclimate have demonstrated significant impact on temperature. A study in Oregon, USA, showed that the air temperature in a campus park was a mean of 5.8 °K cooler than the nearby asphalt car parking area during July and August (Taleghani et al., 2014). The same study reports the cooling impact of vegetation and water within a bare courtyard as 1.6 °K and 1.1 °K respectively (Taleghani et al., 2014). A similar study in Salford, UK, carried out between May and October 2017, measured air temperature differences between a park and an asphalt car parking area. On the hottest summer day, the maximum air temperature difference was 3.6 °K during mid-afternoon. On average, the park was 1.1 °K cooler than the parking lot during three days of a heat wave episode (Taleghani et al., 2019).

Meta studies of measured data summarise that the air temperature at UGI sites is between 1–2 °K lower than the surrounding grey spaces (Bowler et al., 2010; Wang et al., 2022; Zhang et al., 2022). There are numerous specific examples of the measured mitigating effects of parks in particular. Ground level observations from small parks in high-density cities have shown mean reductions in air temperature of between 1.1 °K and 2.9 °K, with the difference being as high as 4.5 °K in Ghardaïa, Algeria, and 6 °K in Sacramento, USA (Lin et al., 2017). UK studies have recorded a large urban park in London being 2.5 °K cooler on average than surrounding areas, and 4 °K cooler in peak summer conditions (Doick et al., 2014). A relatively low measured mean reduction was measured in Glasgow, Scotland, of 0.4 °K (Emmanuel & Loconsole, 2015). Lower values have been reported for a park in Stockholm, with differences of 0.5–0.8 °K during the day, reaching a peak of 2 °K at dusk (Jansson et al., 2007). Size and shape of urban green space influence its cooling effect, and these can reduce with distance away from the UGI (Vaz Monteiro et al., 2016). Even air around isolated street trees has been shown to be between 0.2–0.3 °K cooler than grey space in central Montreal (Wang & Akbari, 2016). It has however been calculated that at least 16% tree cover is

required before a reduction of 1 °K in average air temperature can be achieved; this was quantified using the data-driven model cited above that evaluated microclimate regulation of UGIs in 601 cities across Europe (Manes et al., 2016). The previously cited study that used the MSPA method to characterise urban morphology emphasised the importance of shape and quality of green space for UHI mitigation, citing the orderly nature of the boundary shape of Central Park in New York as an example of how the cooling effects of urban green spaces can be optimised (Lin et al., 2024). It was also demonstrated that land surface temperature could be mitigated through the use of less dense ‘scattered’ urban development incorporating less dense built up areas with moderate high-quality green areas.

3. Methodology

Bluetooth enabled air temperature sensors were used in this work, that record air temperature to an accuracy of ± 0.3 °C (Blue Maestro, 2021). The air temperature sensors are manufactured by Blue Maestro using the product name ‘Disc Mini 003’. These units house a monolithic integrated air temperature and humidity sensor within a polycarbonate casing. Integrated sensor units are manufactured by Silicon Laboratories Inc. using the product name Si7020-A20 and the modules will operate within their defined accuracy range between -10 °C and 85 °C. Silicon Laboratories’ Si7020-A20 sensor modules are factory-calibrated, with the calibration data stored in the on-chip non-volatile memory of the module; this means that recalibration is not required on assembly (Blue Maestro, 2021). The Disc Mini 003 sensors were all housed inside commercially available plastic Stevenson screens to protect the measurements from direct solar radiation, which affects the accuracy of air temperature observations.

Following permission from Leeds City Council (LCC), the Stevenson Shields and sensors were either fixed to street furniture (mainly upright poles of road signs) or hung from trees. Sensors were divided between city centre locations (with 1.5 km of Leeds City Hall), and then at radii of 3 km, 4.5 km and 6 km from this central location. Sensors outside of the city centre were installed near intersects of each radius and the cardinal and ordinal directions. Wherever possible, at each intersect, a sensor was installed in a grey and a green area. Apposite locations on either street furniture or in trees were first identified through a desktop survey using Google Street View. The screens housing the sensors

were secured using heavy-duty plastic cable ties at a height of between 2.5–3.5 m. Co-ordinates were recorded for each sensor location and shared with LCC, along with a series of images illustrating the exact location and fixing. A range of metadata for each sensor location was also recorded to inform the analysis presented in the results section of this paper. These metadata are noted in Table 1 and included: the official

land use designation; the material category of the space (grey or green); the asset it was attached too; the radii distance; and the sector of the city (for example North-East at 6 km).

Relative locations of each sensor and images of typical installs are shown in Figure 1, with sensor locations detailed in Table 1; example images have been annotated for city centre suburban and rural locations. As the

Table 1. Sensor locations and metadata

Sensor	Radius	Sector	Co-ordinates	Elevation	Asset	Space	Land use
LBU001	<1.5 km	City Centre	53.791, -1.554	29 m	Road sign	Grey	Urban
LBU002	<1.5 km	City Centre	53.792, -1.548	31 m	Road sign	Grey	Urban
LBU003	<1.5 km	City Centre	53.800, -1.549	52 m	Road sign	Grey	Urban
LBU004	<1.5 km	City Centre	53.798, -1.551	42 m	Tree (Park)	Green	Park
LBU005	<1.5 km	City Centre	53.798, -1.549	46 m	Road sign	Grey	Urban
LBU006	<1.5 km	City Centre	53.795, -1.544	46 m	Road sign	Grey	Urban
LBU007	<1.5 km	City Centre	53.795, -1.534	30 m	Road sign	Grey	Urban
LBU008	<1.5 km	City Centre	53.803, -1.537	47 m	Tree (Park)	Green	Park
LBU009	<1.5 km	City Centre	53.796, -1.547	52 m	Tree	Green	Urban
LBU010	<1.5 km	City Centre	53.797, -1.543	48 m	Tree	Green	Urban
LBU011	<1.5 km	City Centre	53.801, -1.556	52 m	Tree (Park)	Green	Park
LBU012	<1.5 km	City Centre	53.800, -1.557	46 m	Road sign	Grey	Urban
LBU013	>1.5 km, <3 km	North	53.815, -1.545	45 m	Road sign	Grey	Urban
LBU014	>1.5 km, <3 km	North	53.816, -1.547	65 m	Tree (Wood)	Green	Woodland
LBU015	>3 km, <4.5 km	North	53.828, -1.546	119 m	Road sign	Grey	Urban
LBU016	>3 km, <4.5 km	North	53.824, -1.553	106 m	Tree (Park)	Green	Park
LBU017	>4.5 km, <6 km	North	53.840, -1.548	128 m	Tree (Park)	Green	Park
LBU018	>6 km	North	53.851, -1.545	151 m	Road sign	Grey	Urban
LBU019	<1.5 km	North-West	53.811, -1.562	86 m	Tree (Park)	Green	Park
LBU020	>3 km, <4.5 km	North-West	53.819, -1.581	84 m	Road sign	Grey	Urban
LBU021	>3 km, <4.5 km	North-West	53.823, -1.594	92 m	Tree (Park)	Green	Park
LBU022	>4.5 km, <6 km	North-West	53.830, -1.586	97 m	Road sign	Grey	Park
LBU023	>4.5 km, <6 km	North-West	53.827, -1.589	111 m	Tree (Wood)	Green	Woodland
LBU024	>6 km	North-West	53.836, -1.619	83 m	Road sign	Grey	Urban
LBU025	>1.5 km, <3 km	West	53.802, -1.570	34 m	Road sign	Grey	Urban
LBU026	>1.5 km, <3 km	West	53.802, -1.582	51 m	Tree (Wood)	Green	Woodland
LBU027	>3 km, <4.5 km	West	53.800, -1.592	75 m	Tree (Park)	Green	Park
LBU028	>4.5 km, <6 km	West	53.799, -1.620	96 m	Road sign	Grey	Urban
LBU029	>6 km	West	53.803, -1.641	97 m	Road sign	Grey	Urban
LBU030	>1.5 km, <3 km	South-West	53.790, -1.563	3 m	Road sign	Grey	Urban
LBU031	>1.5 km, <3 km	South-West	53.793, -1.569	35 m	Tree (Park)	Green	Park
LBU032	>3 km, <4.5 km	South-West	53.786, -1.581	72 m	Tree (Park)	Green	Park
LBU033	>4.5 km, <6 km	South-West	53.766, -1.603	78 m	Road sign (Farm)	Grey	Urban
LBU034	>6 km	South-West	53.755, -1.622	156 m	Road sign	Grey	Urban
LBU035	>1.5 km, <3 km	South	53.787, -1.552	34 m	Road sign	Grey	Urban
LBU036	>1.5 km, <3 km	South	53.787, -1.558	40 m	Tree	Green	Urban
LBU037	>3 km, <4.5 km	South	53.772, -1.548	52 m	Road sign	Grey	Urban
LBU038	>3 km, <4.5 km	South	53.770, -1.552	57 m	Tree (Park)	Green	Park
LBU039	>4.5 km, <6 km	South	53.750, -1.555	141 m	Tree (Park)	Green	Park
LBU040	>6 km	South	53.738, -1.547	129 m	Road sign	Grey	Urban
LBU041	>1.5 km, <3 km	South-East	53.788, -1.526	28 m	Fence	Grey	Urban
LBU042	>1.5 km, <3 km	South-East	53.790, -1.525	38 m	Fence	Grey	Urban
LBU043	>4.5 km, <6 km	South-East	53.768, -1.503	25 m	Road sign	Grey	Urban
LBU044	>6 km	South-East	53.763, -1.470	40 m	Tree (Park)	Green	Park
LBU045	>1.5 km, <3 km	East	53.799, -1.527	42 m	Road sign	Grey	Urban
LBU046	>3 km, <4.5 km	East	53.800, -1.503	73 m	Road sign	Grey	Urban
LBU047	>3 km, <4.5 km	East	53.795, -1.507	61 m	Tree (Park)	Green	Park
LBU048	>4.5 km, <6 km	East	53.799, -1.480	40 m	Road sign	Grey	Urban
LBU049	>4.5 km, <6 km	East	53.798, -1.471	76 m	Tree (Park)	Green	Park
LBU050	>6 km	East	53.807, -1.452	80 m	Road sign	Grey	Urban
LBU051	>1.5 km, <3 km	North-East	53.811, -1.523	40 m	Road sign	Grey	Urban
LBU052	>1.5 km, <3 km	North-East	53.814, -1.524	52 m	Tree	Green	Park
LBU053	>3 km, <4.5 km	North-East	53.818, -1.516	52 m	Road sign	Grey	Urban
LBU054	>3 km, <4.5 km	North-East	53.820, -1.522	75 m	Tree (Park)	Green	Park
LBU055	>4.5 km, <6 km	North-East	53.824, -1.507	85 m	Road sign (Wood)	Grey	Urban
LBU056	>4.5 km, <6 km	North-East	53.823, -1.505	95 m	Tree (Wood)	Green	Woodland
LBU057	>6 km	North-East	53.836, -1.501	117 m	Tree (Park)	Green	Park

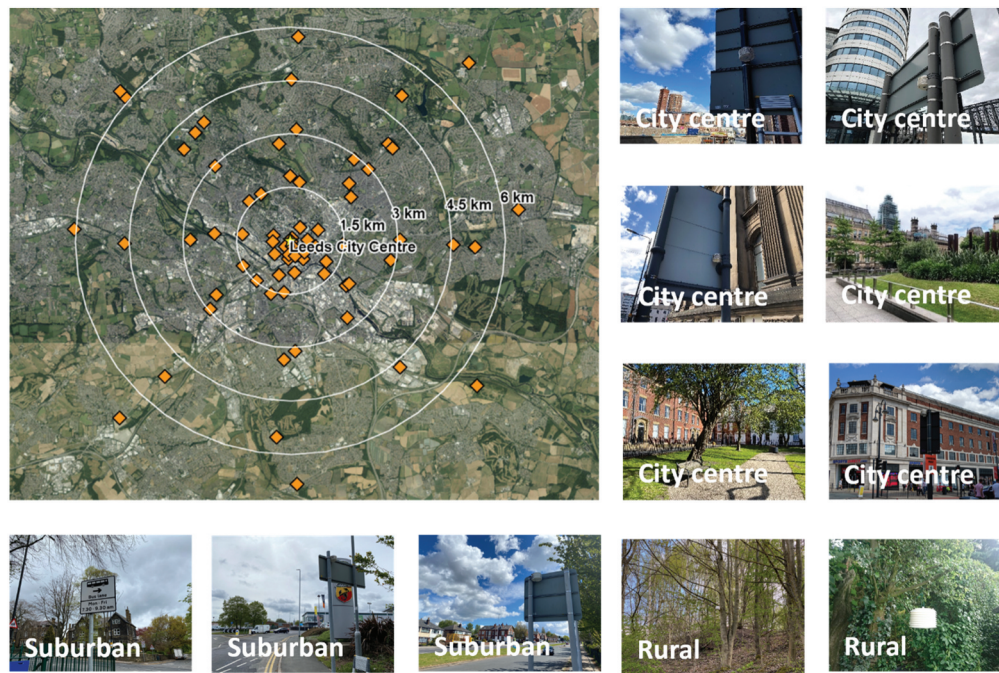


Figure 1. Sensor locations and example installation sites (Contains OS data © crown Copyright and database rights 2023 Ordnance survey [100025252]).

sensors used Bluetooth technology to transmit data to a nearby device, it was necessary to visit each sensor to download data at scheduled periods. Sensors recorded air temperature at 15-minute intervals, and these readings are averaged per hour to produce the hourly dataset used in this work. Unfortunately, there were multiple failures at various sites during the intended monitoring period. Analysis of data collected between the dates of 7 May 2021 and 25 August 2021 is described in this paper. This represents the only period for which a full interrupted dataset for all sensors was available, periods before and after these dates were excluded due to the extent of missing data at numerous sites. It is however a significant sample, with measurements taken every hour across the 57 sites, producing 151,848 data points. These data for the defined period did not include any missing observations, and boxplots were used to visually check for obvious erroneous outlying observations, although no outliers were detected in the reported period. This represents a unique type of dataset at this spatial and temporal resolution that is designed specifically to understand this range of UGI in a city of this scale. Previous work in Manchester and Birmingham used networks of 59 and 82 sensors respectively, to measure UHI effects only, without a specific focus on the UGI areas (Azevedo et al., 2016; G. Levermore & Parkinson, 2016). Numerous studies of green space microclimate

are reported in review papers but reported studies do not use the same scale and resolution of the network described in this work (Bartesaghi Koc et al., 2018; Bowler et al., 2010).

Elevation of the sensor site ranged from between 156 m above sea level at the highest point to the north-west of the city, down to 25 m within the river valley to the south-east of the city centre. In total, 32 of the sensors were attached to street furniture, all of these were areas categorised as grey due their proximity to at least one road and one building. However, one of these sites was largely surrounded by farmland, and another was on the edge of a small wood. Another 25 sensors were hung from trees, 17 of these were in parks, 4 were in urban woods and the remaining 4 were in individual trees within the city centre. The last 2 of the 57 sensors were installed on fences in private gardens. Therefore, in total, 25 sensors were installed in green spaces spread across the city centre and suburbs.

The UHII was calculated by determining a mean hourly value for all sites within a 1.5 km radius of Leeds City Hall, which represents the densely built-up, compact city centre area. Mean hourly values were then calculated for the eight rural reference sites located outside of a 6 km radius from the city centre; these sites are also outside of the Leeds city council boundary. For each hourly timestep, the mean air temperature value from

the rural sites was subtracted from the mean value for the city centre to calculate the UHII. The UHII values for lower resolution time steps, including the daily, monthly and full monitoring period, were quantified by calculating a mean from the hourly UHII values.

Observations made using the air temperature sensors were analysed in the context of local meteorological conditions from the same period of time. These data were acquired from the Copernicus Programme ERA5 hourly datasets (Hersbach et al., 2023). The air temperature data included in this dataset were used in the comparison of air temperature within the different areas of the UHI; to provide a comparison with the ground-level observations, the ERA5 UHII using The weather data published uses the reanalysis technique that combines modelled weather data with historic observations. This allows for original estimates of hourly weather conditions to be refined to provide complete datasets across the globe (Hersbach et al., 2023). Solar radiation, cloud cover and wind speed taken from the dataset for the grid square Latitude 53.75 North—Longitude – 1.5 East (which cover the city of Leeds) have been used to interpret the hourly data measured using the previously described network of air temperature sensors.

In addition to the UHI analysis, the ERA5 weather data was used to calculate the UTCI conditions at the different monitoring sites. The hourly UTCI calculation method is described in detail in exiting work (Bröde et al., 2012; Broede et al., 2010; Jacobs et al., 2019). The UTCI takes account of the thermoregulation of the human body to describe physiological comfort conditions when subjected to a range of meteorological variables including relative humidity, wind speed and direction, and solar radiation (Bröde et al., 2012). Four weather variables are required to calculate the UTCI: air temperature, dew point temperature or relative humidity (relative humidity is used in this work), wind speed at 10 m above ground, and mean radiant temperature (Bröde et al., 2012). A UTCI calculator was used for the hourly values reported in this work (Lemke, 2010). All required weather variable data were acquired through the ERA5 datasets noted above; to calculate the mean radiant temperature, it is necessary to use solar radiation data following a calculation method defined in (Ramsey & Bernard, 2000). Results are categorised into ten stress categories that range from extreme cold stress up to extreme heat stress (Blazejczyk et al., 2013).

4. Results and discussion

4.1. Leeds urban heat island May 2021–August 2021

Mean diurnal profiles of air temperature within the city centre, suburbs and rural reference sites are shown in

Chart (a) of Figure 2, along with the air temperature profile from the ERA5 regional dataset. The mean values for the local sensor network were created by calculating a combined mean hourly value of all city centre sites, the suburban areas (between 1.5 km and 6 km from the city centre) and the reference sites (greater than 6 km from the city centre), independent of land use or land cover. Although the summer of 2021 was relatively cooler in Leeds than in other recent years, the UHI effect can be seen between the profiles, with its greater prevalence at night-time visible. Within this data set, the peak temperature recorded was 32.8 °C, with a mean temperature across all sites of 15.4 °C; the mean temperature for the hottest 7-day period was 21.4 °C (15 July –21st July). In many studies of UHIs, a single rural reference site is used to calculate the UHI intensity (UHII—the difference between city centre and rural temperature). This is however simplistic and does not capture the complexity of each city's layout, land cover and topography. A summary of maximum, mean and minimum temperatures for all sensor locations is presented in Table 2.

When using only the reference sites that are over 6 km in distance from the city centre to calculate the UHII, the mean for the whole monitoring period was 0.8 °K, with the peak hourly mean value of 1.4 °K occurring at 02:00 over night. The peak individual hour UHII for the mean of sites along the 6 km radius over the entire period was 3.1 °K, which was recorded at 03:00 on 16 June 2021. Profiles before and after this peak are shown in Chart (b) of Figure 2; data for these dates have been included to help illustrate absolute values rather than mean hourly values from the entire monitoring period. When compared to the regional air temperature value in the ERA5 dataset, this peak reaches 3.9 °K. Higher nighttime air temperature can cause disruption to sleep and exacerbate poor health conditions; this is particularly relevant in a city like Leeds as domestic properties are most commonly reliant on natural ventilation for cooling. This problem can also be made worse by security concerns in inner city areas, as residents may not be comfortable leaving windows open overnight. For air conditioned buildings, the warmer nighttime conditions lead to an increase in energy consumption and heat rejection from chillers also add to urban heating.

If all of the suburban sites outside of the city centre 1.5 km radii are included in the calculation, then the average UHII is only 0.6 °K, and the peak is 2.1 °K. The city centre of Leeds is relatively dense and high-rise, but then becomes more dispersed and low-rise past the 1.5 km radius from the city centre. The relative differences between UHII intensities are therefore indicative of these changes in land cover. The mean UHII of 0.6 °K

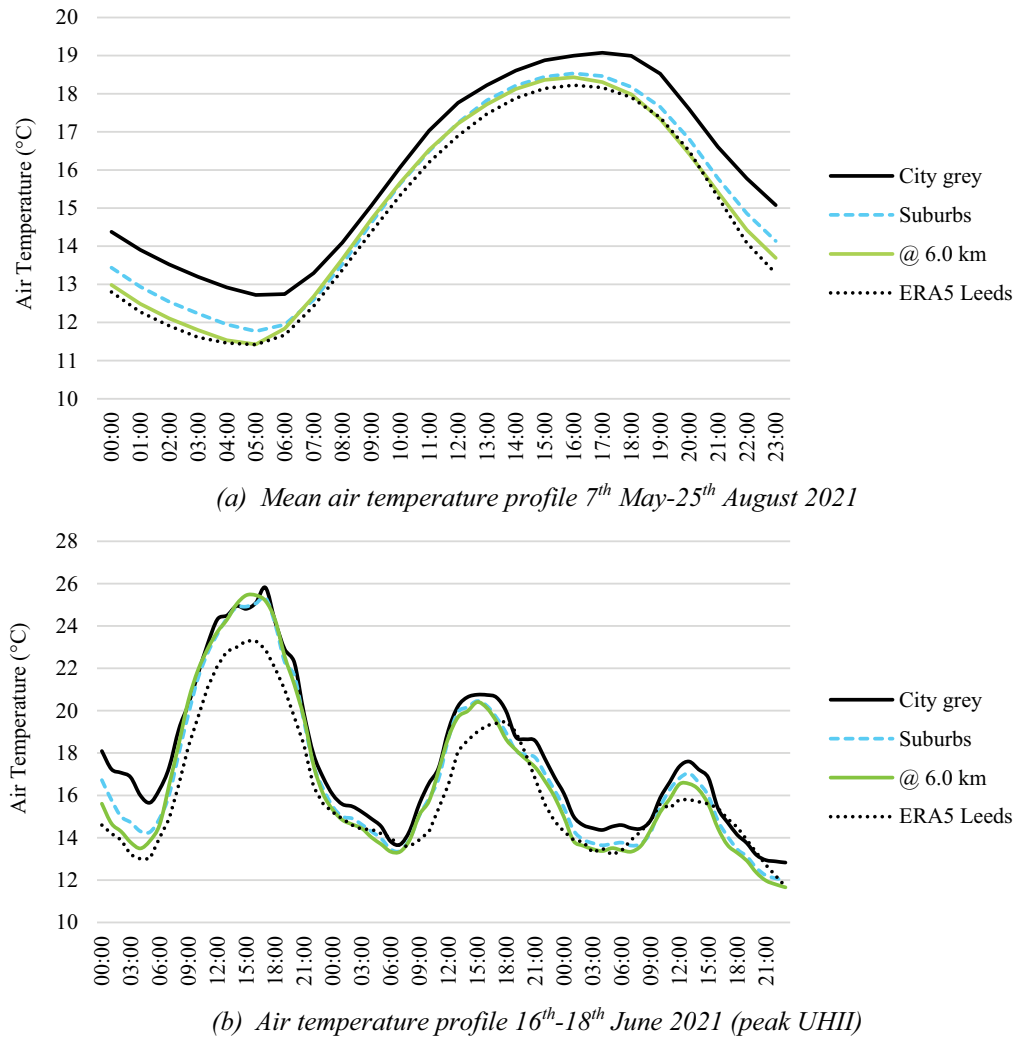


Figure 2. Mean diurnal air temperature profiles.

for this period reflects the range of reference sites, and is lower than the mean value of 1.2 °K during summer 2013 reported for Leeds in previous work (Parker, 2021). The mean and peak values in this dataset are also lower than those reported for Birmingham, Manchester and London in the UK, with the summertime peak being considerably lower than the peak UHII values of 7 °K and 8 °K for those cities respectively (Azevedo et al., 2016; Levermore & Parkinson, 2016; Watkins et al., 2002). There are two main likely differences between these other UK cities and Leeds, they all have larger dense city centre areas, and the summer period considered in this work was relatively cool compared to the hottest years, which reduces the magnitude of difference. Additionally, the morphology of the city areas is different and future analysis would benefit from the use of the MSPA technique cited in the literature review section (Lin et al., 2024) as this would allow for these differences to be quantified.

Monthly mean hourly profiles of the calculated UHII are illustrated in Figure 3. The magnitude of UHII does increase slightly during the warmer months of summer 2021 but the diurnal pattern of the UHII is similar for all observed periods. During the summer of 2021, 21 July was the warmest month with a mean air temperature of 18.2 °C in the city centre and 17.6 °C across all of the rural reference sites. The pattern of the UHII is consistent with the understanding of heat island effects in the UK, with daytime air temperature being similar between the urban and rural sites. Warmer air temperature is then maintained overnight due to the thermal mass in the denser urban areas. The consistency of the monthly UHII patterns is reflected in the mean value for each month being 0.8 °K for May and June, increasing slightly to 0.9 °K for July and August. A similar proportion of observed hours exceeded a UHII of 1 °K in all months, 31 % in May, 32 % in June, 37 % in July and 38 % in August. The proportion of observed hours

Table 2. Summary of air temperature observations for all sensor locations

Sensor	Radius	Sector	Elevation	Land use	Air temperature (°C)		
					Maximum	Mean	Minimum
LBU001	<1.5 km	City Centre	29 m	Urban	31.0	16.0	2.5
LBU002	<1.5 km	City Centre	31 m	Urban	30.4	15.8	2.9
LBU003	<1.5 km	City Centre	52 m	Urban	28.9	15.7	3.5
LBU004	<1.5 km	City Centre	42 m	Park	29.2	15.7	2.9
LBU005	<1.5 km	City Centre	46 m	Urban	30.2	16.1	3.3
LBU006	<1.5 km	City Centre	46 m	Urban	32.6	16.3	3.5
LBU007	<1.5 km	City Centre	30 m	Urban	28.7	15.8	2.5
LBU008	<1.5 km	City Centre	47 m	Park	27.9	15.2	2.6
LBU009	<1.5 km	City Centre	52 m	Urban	30.4	16.0	3.5
LBU010	<1.5 km	City Centre	48 m	Urban	29.3	16.2	3.9
LBU011	<1.5 km	City Centre	52 m	Park	29.2	15.5	2.1
LBU012	<1.5 km	City Centre	46 m	Urban	30.6	16.0	2.9
LBU013	>1.5 km, <3 km	North	45 m	Urban	31.3	15.8	0.5
LBU014	>1.5 km, <3 km	North	65 m	Woodland	27.3	14.7	1.6
LBU015	>3 km, <4.5 km	North	119 m	Urban	31.0	15.0	1.8
LBU016	>3 km, <4.5 km	North	106 m	Park	27.7	14.5	1.5
LBU017	>4.5 km, <6 km	North	128 m	Park	27.0	14.5	2.0
LBU018	>6 km	North	151 m	Urban	29.9	14.9	1.9
LBU019	<1.5 km	North-West	86 m	Park	28.5	14.8	1.8
LBU020	>3 km, <4.5 km	North-West	84 m	Urban	30.7	15.6	2.1
LBU021	>3 km, <4.5 km	North-West	92 m	Park	28.7	14.7	1.3
LBU022	>4.5 km, <6 km	North-West	97 m	Park	28.6	15.1	1.1
LBU023	>4.5 km, <6 km	North-West	111 m	Woodland	28.1	14.6	1.5
LBU024	>6 km	North-West	83 m	Urban	30.1	15.1	-0.5
LBU025	>1.5 km, <3 km	West	34 m	Urban	30.2	15.9	2.0
LBU026	>1.5 km, <3 km	West	51 m	Woodland	27.5	15.0	1.8
LBU027	>3 km, <4.5 km	West	75 m	Park	28.5	14.9	1.9
LBU028	>4.5 km, <6 km	West	96 m	Urban	31.8	15.6	1.2
LBU029	>6 km	West	97 m	Urban	31.6	15.7	1.7
LBU030	>1.5 km, <3 km	South-West	3 m	Urban	31.0	15.9	1.8
LBU031	>1.5 km, <3 km	South-West	35 m	Park	28.5	15.3	1.7
LBU032	>3 km, <4.5 km	South-West	72 m	Park	27.7	14.9	1.9
LBU033	>4.5 km, <6 km	South-West	78 m	Urban	29.9	14.9	-0.6
LBU034	>6 km	South-West	156 m	Urban	30.7	15.1	2.2
LBU035	>1.5 km, <3 km	South	34 m	Urban	31.5	15.9	1.7
LBU036	>1.5 km, <3 km	South	40 m	Urban	28.1	15.2	2.6
LBU037	>3 km, <4.5 km	South	52 m	Urban	31.9	16.2	2.3
LBU038	>3 km, <4.5 km	South	57 m	Park	28.1	15.1	2.5
LBU039	>4.5 km, <6 km	South	141 m	Park	27.3	14.4	2.0
LBU040	>6 km	South	129 m	Urban	29.6	14.9	2.4
LBU041	>1.5 km, <3 km	South-East	28 m	Urban	28.7	15.7	2.7
LBU042	>1.5 km, <3 km	South-East	38 m	Urban	31.9	16.1	2.8
LBU043	>4.5 km, <6 km	South-East	25 m	Urban	31.5	15.8	1.1
LBU044	>6 km	South-East	40 m	Park	28.4	14.5	0.6
LBU045	>1.5 km, <3 km	East	42 m	Urban	30.9	15.8	2.0
LBU046	>3 km, <4.5 km	East	73 m	Urban	32.4	15.8	1.9
LBU047	>3 km, <4.5 km	East	61 m	Park	28.2	15.2	2.7
LBU048	>4.5 km, <6 km	East	40 m	Urban	30.1	15.5	0.2
LBU049	>4.5 km, <6 km	East	76 m	Park	27.8	14.9	2.2
LBU050	>6 km	East	80 m	Urban	30.9	15.6	1.4
LBU051	>1.5 km, <3 km	North-East	40 m	Urban	32.8	16.1	1.4
LBU052	>1.5 km, <3 km	North-East	52 m	Park	29.4	15.6	1.9
LBU053	>3 km, <4.5 km	North-East	52 m	Urban	31.8	16.2	0.9
LBU054	>3 km, <4.5 km	North-East	75 m	Park	27.7	14.8	1.5
LBU055	>4.5 km, <6 km	North-East	85 m	Urban	31.0	15.1	0.9
LBU056	>4.5 km, <6 km	North-East	95 m	Woodland	26.5	14.3	1.6
LBU057	>6 km	North-East	117 m	Park	27.8	14.5	1.8

exceeding a UHII of 2 °K was greater in June at 20 %, reflecting the trend in the early hours, with values similar for all other months (7 % in May and August, and 8% in July). When comparing the magnitude of the UHII with the mean daily air temperature, in most instances, the UHII is greater on cooler days as illustrated in Figure 4. This is due to the air temperature on hotter days being similar in both rural and central urban areas

during the longer daylight hours. This comparison also emphasises the need to measure a high temporal resolution where possible, so that the diurnal pattern of the UHII can be understood.

When determining the UHII for any city, in addition to considering land cover, it is important to consider the elevation and topology the reference sites used in the calculation, as identified using a smaller

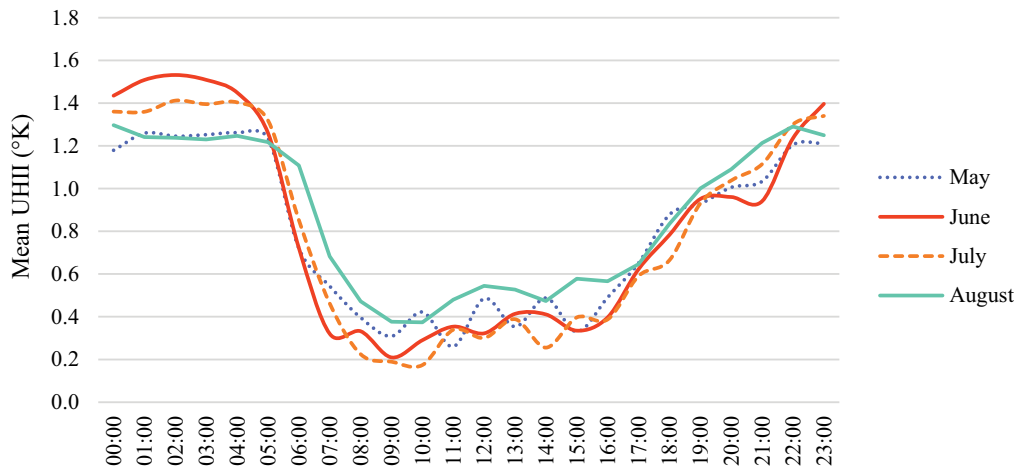


Figure 3. Monthly mean diurnal UHII profiles.

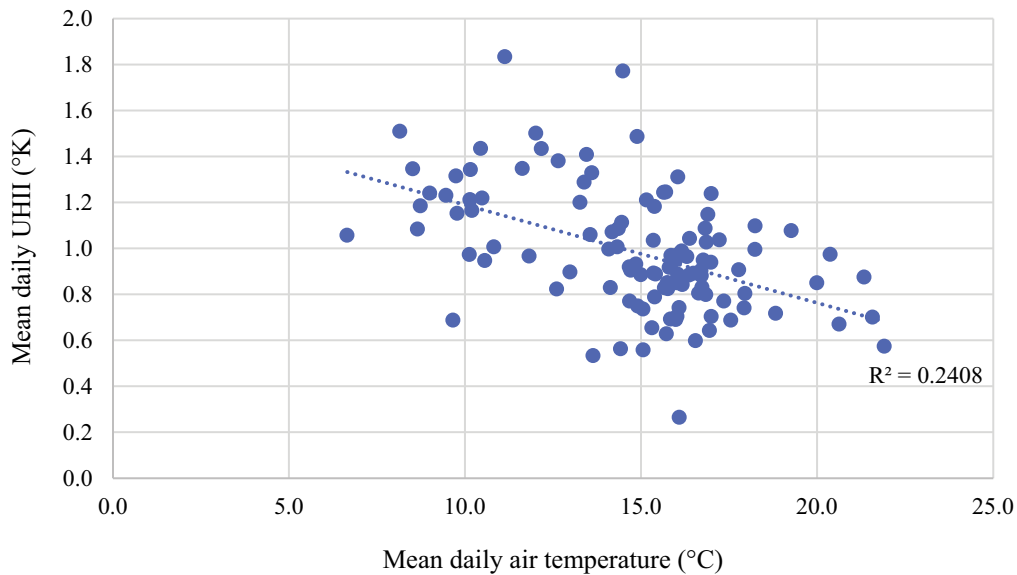


Figure 4. Comparison between mean daily air temperature and mean daily UHII.

sample set in previous work (Parker, 2021). The importance of considering the site elevation is emphasised in Figure 5, which illustrates the average air temperature for sites within different elevation ranges. The data indicate a linear relationship between temperature and elevation, with lower temperature at higher elevation, although this was somewhat affected at a local scale by land cover. Using average air temperature over the whole monitoring period, the sites in the highest elevation range are approximately 1.1 °K cooler than the lowest.

To provide further context for this analysis, the average UHII compared against eight different reference sites along the 6 km radius from the centre are shown in Figure 6. For each of the reference sites, the location in terms of direction is noted, along

with the site elevation, land use and land cover. Intuitively, it could be expected that the sites at the higher elevations would result in the greatest UHII, although this is not the case in this sample set. Some of the higher mean UHII values were recorded at some of the lower elevations and results shown here also suggest that the land cover at each site influences these observations as well; it is important to note that the two highest values shown here were recorded in green space. Future work could also use the MSPA method to inform further analysis based upon the density and morphology of both the urban and rural sites (Lin et al., 2024). These results emphasise the importance of the reference sites used to calculate UHII for urban canopy air temperature measurements, but also indicate the

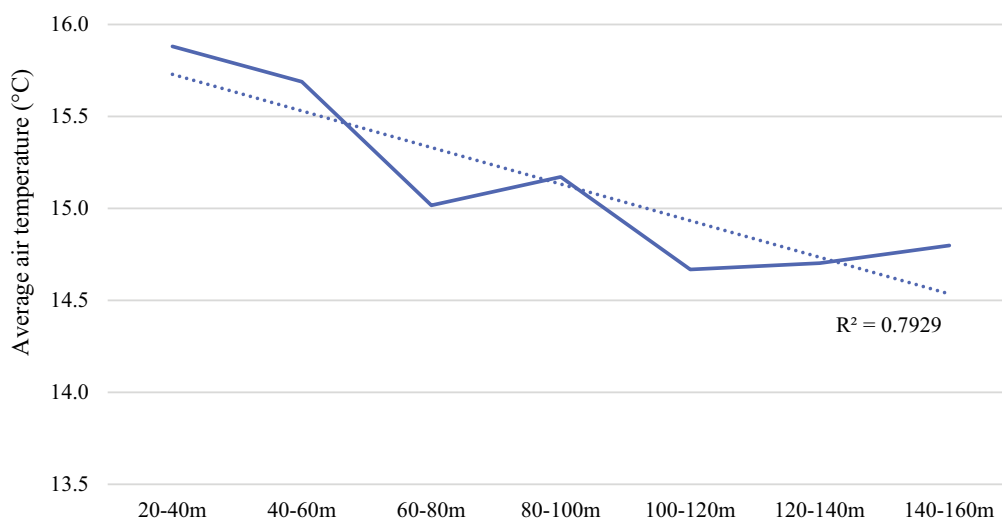


Figure 5. Average air temperature for elevation ranges.



Figure 6. Calculated UHII for different rural reference sites.

limitations of these types of measurement in terms of available monitoring sites, as some sites on the outskirts can still be in built-up areas, even though there are not formally part of the city itself.

As noted previously, mean UHII during the monitoring period is a little lower than those reported in the literature for other cities in the UK. However, Figure 6 suggests that this could be influenced by the range of reference sites used in this calculation. The peak UHII calculated using the mean value from all reference sites was approximately 3 °K lower than found in Birmingham, and 4 °K lower than the measured peaks in both London and Manchester. However, the peak UHII when comparing between the different reference sites shown in Figure 4 ranged from 2.9 °K for the Eastern site and up to 6.6 °K for the North-Western site, a summertime peak similar to those cited in other major UK cities. This could be

influenced by the topography of the city area and the influence of this should be considered in future work; the city area of Leeds encompasses higher elevations and a much greater range of elevations than the other major UK cities discussed in this paper (London, Birmingham and Manchester). Understanding this in greater detail will require more localised instrumentation to observe other weather conditions at the specific reference sites. It is important to note that the outer suburbs can in some instances be significantly warmer than the city centre due to localised cloud cover and wind conditions throughout some days (although these variables were not measured in this study). Although much less frequent, a peak hourly difference of 6.1 °K was recorded at the Northern site; 17 % of the hourly observations at this site were warmer than the average in the city centre over the monitoring period, all of which occurred during daylight hours.

4.2. Comparison of grey and green spaces

4.2.1. Air temperature conditions

Mean difference in air temperature (ΔT) between grey and green spaces was 0.7 °K during the full monitoring period, with an hourly peak ΔT of 2.5 °K occurring at 14:00 on 20 July 2021; the peak in the hourly mean value was 1.2 °K, these being at the opposite time of day from the peak UHII. This suggests that it is mainly the shading effects of the trees in the green spaces that are being captured in these data. Cooler air temperature in green spaces during daylight hours is of more benefit to the city's citizens as they can take advantage of these conditions, especially for people who have health issues that are exacerbated in hot weather, such as cardiovascular and respiratory conditions. Comparing data from parks specifically results in these values going up marginally, with parks being a maximum of 2.6 °K cooler during the day, and 0.8 °K cooler on average across the monitoring period. The mean values are slightly higher than those reported for Glasgow in the UK (Emmanuel & Loconsole, 2015) but significantly lower than the ΔT of the large park areas in London (Doick et al., 2014), although peak reductions are closer than the mean values. Observed lower air temperature in green spaces during the daytime than during the night are also consistent with values reported in the literature. The average diurnal air temperature profiles for all grey and green spaces are compared in Figure 7.

Mean hourly temperature profiles for different categories of green infrastructure are compared in Figure 8. This illustrates the average hourly temperature in the city centre, urban grey spaces (all grey spaces in the centre and suburbs), city centre individual trees, city centre small parks, parks outside of the city centre, and inside treespaces (urban woodland). The y-axis in

Figure 8 has been truncated at 10 to aid visualisation. During day light hours, there is very little difference between the city centre grey spaces, the urban grey spaces across the city, and, notably, the individual trees within the city centre. This suggests that in this context, single trees have very little impact of the air temperature on their own, and that the conditions are influenced by the dense built environment that surrounds them, consistent with one example in the literature (Wang & Akbari, 2016) but not commonly understood. This is important for city planning and urban design as it negates the notion that individual trees will cool spaces on their own. They can provide shade for individuals from direct solar radiation but on this evidence, won't cool down the air around them. Although there is very little difference between the city centre and total urban grey space temperatures during the daylight hours, during the night the air temperature in grey spaces outside of the city centre is on average 0.7 °K cooler than the centre; during the hottest week in this dataset, the peak difference was 1.2 °K at 04:00 on 17 July 2021. These differences between the denser urban centre and suburbs could also be related to morphology as previously discussed (Lin et al., 2024).

As noted above, the mean ΔT between grey spaces and parks was 0.8 °K, with a peak hourly mean of 2.6 °K. However, a mean ΔT of 1.3 °K was measured between a large park in the South of the city along the 4.5 km radius; the peak hourly ΔT between urban grey spaces and this park was 4.9 °K, occurring at 19:00 on 9 August 2021. Four small city centre parks were included in this sample set, and the mean ΔT for these spaces was 0.5 °K, with an hourly peak of 1.8 °K, within the denser urban environment. These findings are consistent with the work describing shape and distribution of green spaces

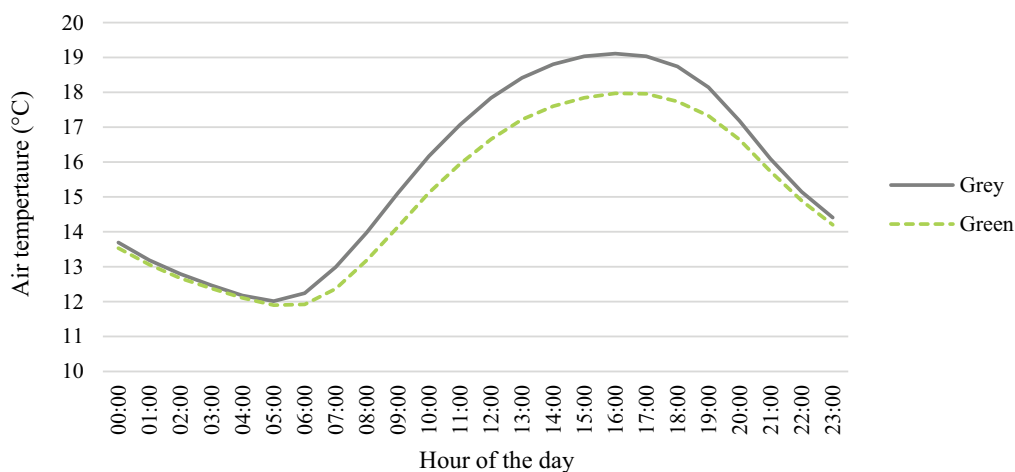
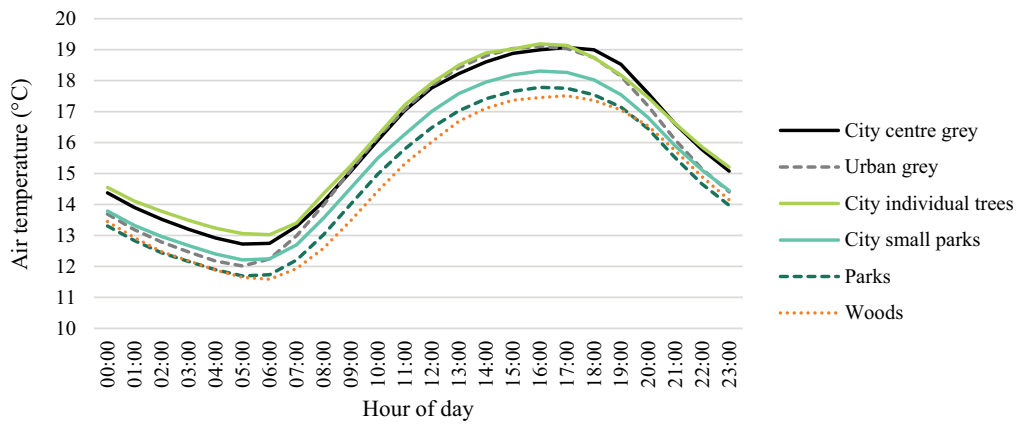
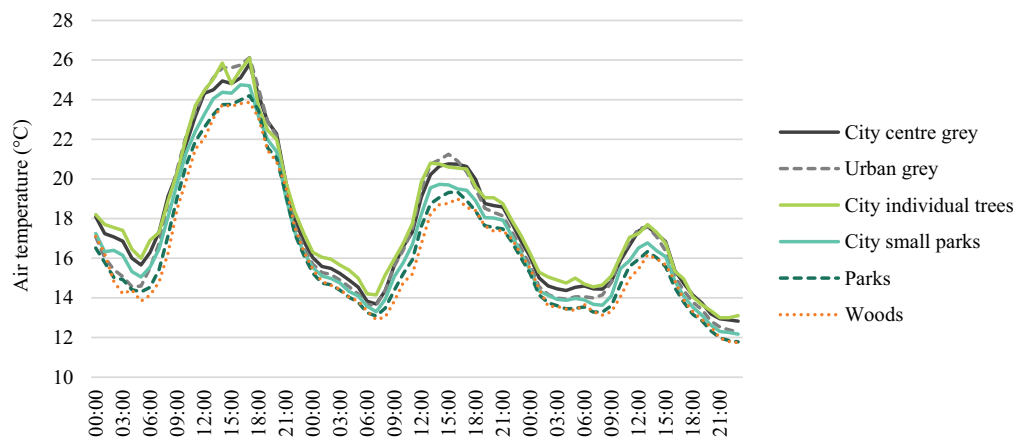


Figure 7. Average diurnal air temperature in grey and green spaces.



(a) Mean air temperature profile in grey and green spaces May-August 2021



(b) Mean air temperature profile in grey and green spaces 16th-18th June 2021 (peak UHII)

Figure 8. Average diurnal air temperature in areas of different land cover.

using the MSPA method to evaluate land surface temperatures (J. Lin et al., 2024). Data reported in this paper could also provide useful cross validation for other

studies such as that noted above, especially for any work aiming to infer air temperature conditions using remote sensing surface temperature data. In contrast,

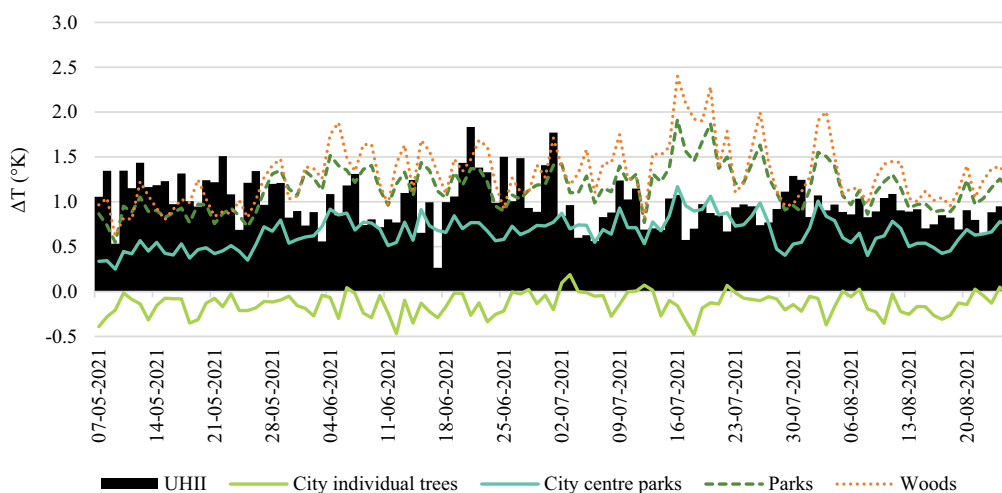


Figure 9. Comparison of mean daily UHII with air temperature differences in grey and green spaces.

another four sensors were installed within treescapes that fall within the city boundaries, the mean ΔT within these spaces was 1.3 °K and the mean hourly peak reached 3.5 °K. Although the vast majority of mean hourly observations show UGI to be consistently cooler (>93% for all categories) the magnitude of this differed between categories. Whilst on average, 26 % of hours were more than 1 °K cooler across all UGIs, this ranged from just 5.5 % of hours in city centre parks to 63 % of hours in the monitored woods. These results suggest that the UGI provides consistently cooler spaces that citizens can utilise during hotter periods; the implications of this in the context of heat stress are discussed in the final subsection of this paper.

Figure 9 illustrates the mean daily air temperature difference (ΔT) for the UHII (comparing city centre with rural reference sites) and differences between grey spaces and the categories of UGI included in this study over the full monitoring period. During the warmer summer months, daily ΔT for the parks and woods is often greater than the UHII, this demonstrates the extent of temperature reduction associated with the larger UGI areas over the small city centre parks, although at a daily resolution, these spaces provide a reduction in heat that is comparable with the UHII, especially during warmer summer months. This has important implications for the protection of existing UGI areas but also for future planning and development. As heatwave periods are forecast to become more frequent and intense in the future, these results demonstrate that larger UGI areas should be prioritised where possible to maximise cooling, but also that increasing the number of smaller city centre parks can also help mitigate future overheating.

4.2.2. Influence of meteorological variables on UGI conditions

Weather conditions have been identified as an important factor that influences the UHI effect in previous work on other cities in the UK (Levermore & Parkinson, 2019; Levermore et al., 2018; Levermore et al., 2015). In particular, higher wind speed has been shown to reduce the UHII as it encourages increased air mixing. Increased cloud cover has also been shown to reduce UHII as greater cloud cover limits the heat exchange related to long-wave radiation, meaning that rural areas cool down at a slower rate than under clear skies overnight (Levermore & Parkinson, 2019; Levermore et al., 2018; Levermore et al., 2015). In this work, wind speed, solar radiation and cloud cover have all been used to contextualise the air temperature observations. As noted

earlier, these weather data were acquired from the ERA5 hourly datasets (Hersbach et al., 2023). Mean ΔT across the full dataset are visualised in Figure 10 for the UHI ΔT , UGI ΔT , City Centre Parks (CCParks ΔT) and Woods ΔT . The values for the UHI ΔT show how much lower temperatures were in the outer suburbs (at 6 km) than the city centre; the UGI ΔT show how much cooler the green spaces were than the mean for urban grey spaces; the CCParks ΔT how much cooler the city centre parks were than surrounding grey space; and the Woods ΔT how much cooler these areas were than urban grey spaces.

The influence of wind speed on the UHI in this dataset is not particularly pronounced, although it does reduce the mean intensity slightly at higher wind speed. All green spaces are cooler than the corresponding grey spaces at lower wind speed, but this is most pronounced for the Woods ΔT , with the mean ΔT at the lowest wind speed being 1.8 °K, which reflects the increased shading and cooling effect on the air within these tree canopy areas compared with the built-up areas around them. This relationship is further illustrated by the chart in Figure 11, with mean daily ΔT values being greater in all UGI under lower wind speeds, with this being more pronounced for the larger parks and woodland. These results again underline the benefit of protecting and expanding these larger assets where possible. For example, new housing developments could be planned to border existing larger UGI, and larger developments could be intersected by smaller UGIs to capitalise upon the inherent cooling of the existing spaces. Similarly, these data could also support the establishment of new smaller UGI in available city centre sites, rather than adding to the already dense built-up environment.

4.2.3. Impact of UGI on human thermal comfort

In order to understand the relevance of air temperature differences to human comfort, hourly UTCI values for the different categories of UGI and grey spaces were calculated. The UTCI metric describes how people experience atmospheric conditions and provides an equivalent temperature metric (°C) that defines levels of thermal stress. Categories of thermal stress are defined as follows: above + 46: extreme heat stress; +38 to + 46: very strong heat stress; +32 to + 38: strong heat stress; +26 to + 32: moderate heat stress; +9 to + 26: no thermal stress; +9 to 0: slight cold stress; 0 to - 13: moderate cold stress; -13 to - 27: strong cold stress; -27 to - 40: very strong cold stress; below - 40: extreme cold stress (Bröde et al., 2012). The UTCI is a well-established metric commonly used in thermal comfort

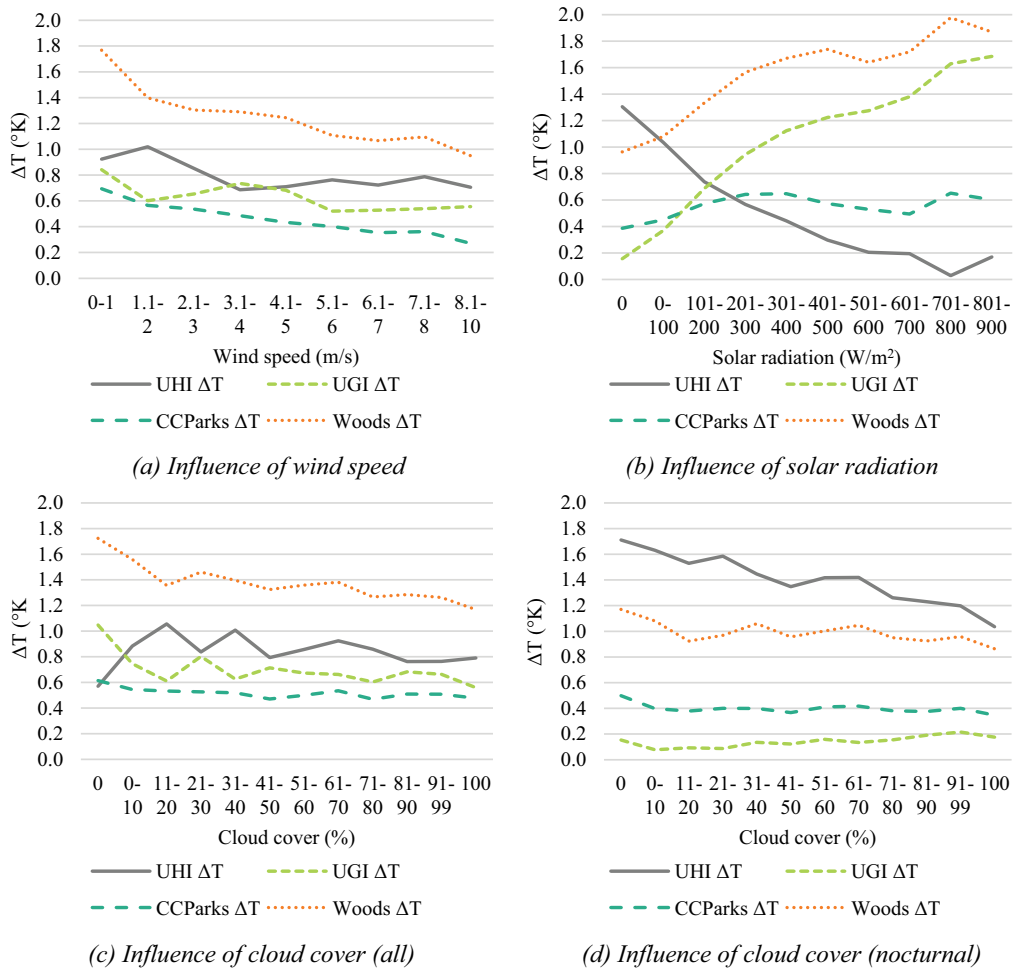


Figure 10. Influence of weather variables on air temperature differences between grey and green spaces.

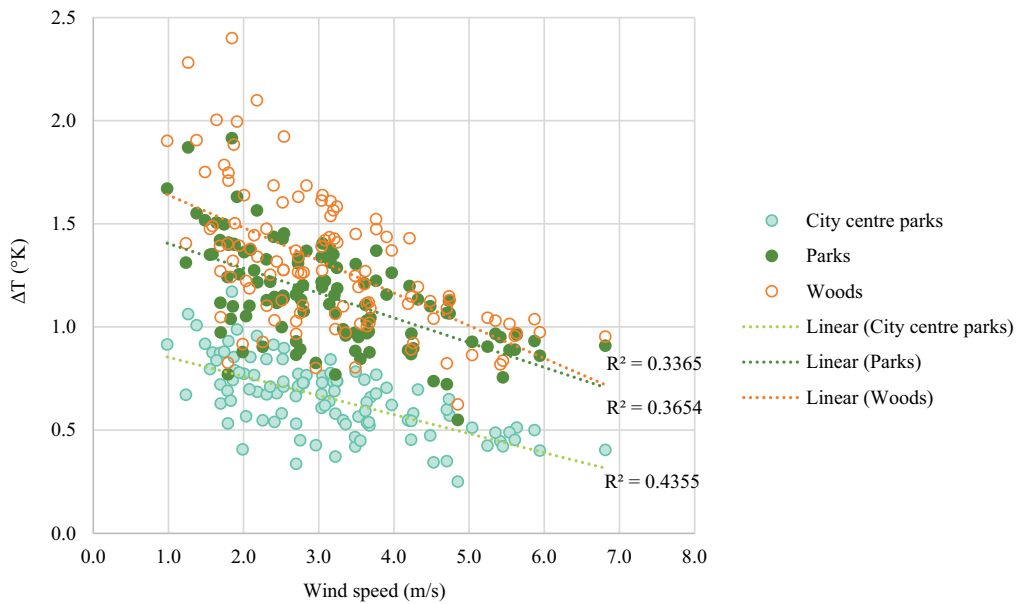
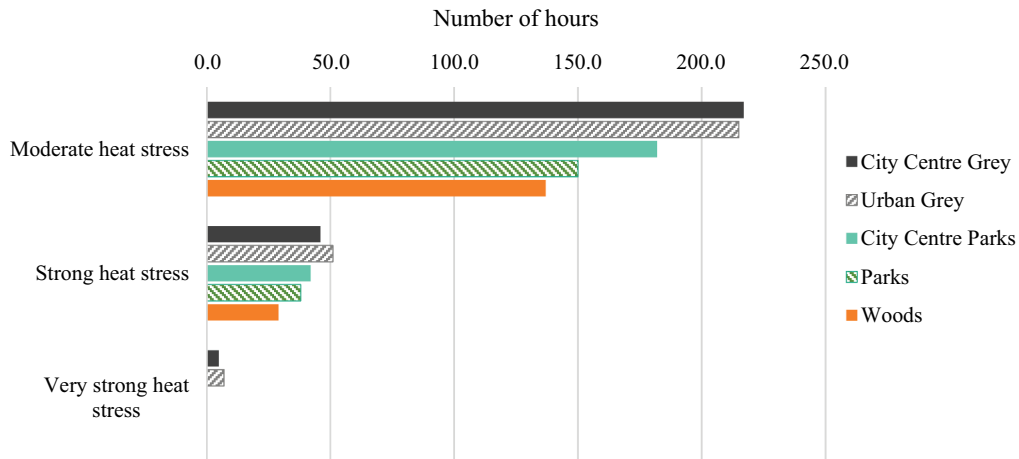


Figure 11. Relationship between mean daily air temperature differences and wind speed.

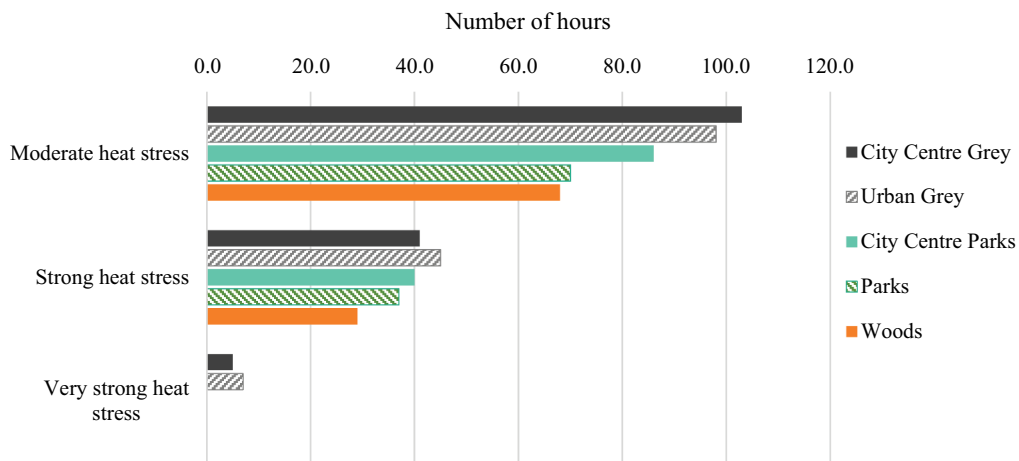
studies (DiNapoli et al., 2021; Jacobs et al., 2019). Dynamic heat exchanges between humans and the environment are accounted for in the calculation, considering physiological response and clothing adaptation in different meteorological conditions (Bröde et al., 2012). Meteorological inputs required for the calculation include air temperature, relative humidity, wind speed and solar radiation. It is important to note that it is only the inputs for air temperature that have been adjusted for the specific types of space in this work; remaining inputs are taken from the ERA5 regional dataset for Leeds over the same period (Hersbach et al., 2023). The UTCI values presented here are therefore indicative of average conditions in the grey and green spaces and could be refined further using localised observations of relative humidity, wind speed and solar radiation. Results are however a useful indication

of the impact of different environments on human comfort.

The number of hours considered to be under heat stress are illustrated in Figure 12, presenting values for the full dataset (a) and the hottest month of July (b). Although the summer of 2021 in Leeds was relatively mild, it is still possible to quantify the comfort benefits of the green spaces from these data. The mild conditions during the monitoring period are reflected by the majority of observed hours being categorised as being under no thermal stress (greater than 64% for all spaces). It is however possible to conclude that the green spaces subject human beings to lower levels of heat stress than the grey spaces. From the full sample set, >8 % of monitor hours in grey spaces were considered to be under moderate heat stress, which rises to > 13 % of hours during July. This compares with 6.8 % of



(a) UTCI heat stress values for 7th May-25th August 2021



(b) UTCI heat stress values for July 2021 (hottest month)

Figure 12. Universal thermal climate index in grey and green spaces.

hours in small urban parks, 5.6 % of hours in larger parks and 5.1 % of hours in woodland being under moderate heat stress over the full monitoring period. For July, these values increase to 11.6 % in small urban parks, 9.4 % in larger parks and 9.1 % in woods. A similar pattern is evident for hours under strong heat stress, in all cases, people in woods would experience the lowest exposure to heat stress, followed by larger parks. A very small number of hours were considered to be under strong heat stress (<1 %) but these only occurred in the grey spaces. The consistency in these more thermally comfortable conditions throughout the monitoring period is emphasised in Figure 13, where the mean daily difference in UTCI values between grey and green space categories is illustrated.

These results can be used to support the promotion of using these spaces for recreational activities and exercise during heatwaves, especially for at-risk individuals with health issues that are exacerbated by high air temperature. They could be used to support citizen access to these spaces through urban public transportation systems. Using the UTCI metric provides a stronger evidence base for this type of policy and practice information than air temperature differences alone. Further work can be done to measure localised conditions for wind speed and solar radiation in particular as these can have a significant impact on thermal comfort.

5. Conclusion

A high spatial and temporal resolution dataset for the Leeds UHI and UGI air temperatures has been described in this paper, covering the period May 2021–August 2021. The average UHI intensity during the

monitoring period was 0.9 °K which is lower than that reported for other cities in the UK, although previous work from other years has shown the UHII in Leeds to be similar to that found in other major UK cities. In contrast to previous studies, this work demonstrates the importance of using multiple rural reference sites to calculate the UHII, especially in cities with a significant change in elevation across their area. The average UHII for four of the eight rural reference sites was above 1 °K. A summer maximum UHII of 3.1 °K was calculated using the mean values for all city centre and all rural reference sites, occurring in late evening. Although there is variation across the monitoring sites, green space was on average 0.7 °K cooler than the grey spaces during the summer months, and up to 2.6 °K cooler on some of the hottest days; air temperature in an urban wood was over 4 °K cooler on the hottest days. This work contributes to knowledge in this area as 25 of the 57 sensors were deliberately installed within UGI areas, to quantify the differences between air temperature and thermal comfort in grey and green urban areas.

The diurnal pattern of the UHII for Leeds during this monitoring period was similar to other cities in that it is higher during nocturnal hours, although these differences were not as pronounced in this dataset as they are in other examples from the literature. There is a relatively small proportion of green space in Leeds city centre but the small areas of UGI were still an average of 0.2 °K cooler than the surrounding grey space and this can reach a peak of up to 2.5 °K cooler during the hottest days of summer months. Significantly, there was no observable difference between temperatures in grey spaces and individual street trees in the city centre. This shows the importance of dedicated green spaces in

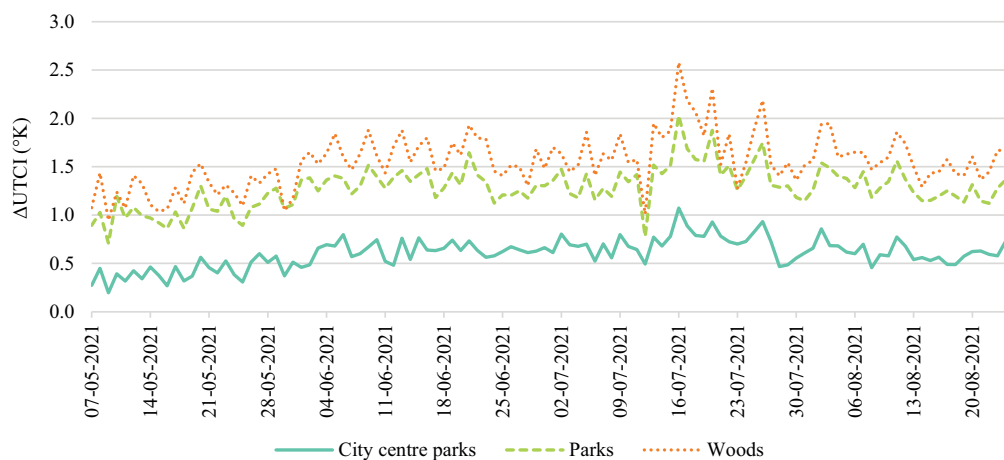


Figure 13. Mean daily UTCI difference between grey and green space categories.

mitigating urban heat and providing relief from more extreme conditions. The majority of hourly air temperature and UTCI values in UGI were lower than the surrounding grey spaces, suggesting that these spaces provide relief from heat stress for the city's residents; this is particularly important for people that experience health issues exacerbated by excessive heat. During many summer days, the mean air temperature in UGI areas was comparative with those observed at the UHI rural reference sites.

The main limitations of this work relate to the sensors used to compile the dataset. Air temperature readings are subject to an error of ± 0.3 °C and future work will aim to deploy more accurate instruments. The Stevenson screens used in this work are commercially available but are not subject to any independent standards and further work will investigate the efficacy of this equipment. Although the relative size of the sensor network is large, this could of course be increased which is another practical limitation of this work. Another obvious limitation to the work is that the monitoring period is limited to the defined summertime period. Whilst this is a specific period of interest in the context of mitigating high summer periods, future work should aim to collect data over longer periods of time; this has practical implications in terms of battery life of the sensors used. Future work will explore technological solutions to monitor for longer periods, it will also aim to monitor in a greater range of green spaces, for example comparing newly established parks with older parks, different types and sizes of urban woods and commercial/private spaces, such as urban farms and domestic gardens,

Despite the noted limitations, this dataset and the associated analysis described here are however potentially useful for a variety of further investigations. In terms of the urban environment, these data are useful for both the modelling and measurement of building performance, overheating analysis, model validation (metrological, building performance and thermal comfort). The results for the UGI impact also have implications for city planning and policy development, which in turn can have long-term impacts on public health and wellbeing. Further work on UTCI analysis will also aim to measure localised relative humidity, wind speed and solar radiation; all of these factors can influence the UTCI calculation and would refine this assessment.

Disclosure statement

No potential conflict of interest was reported by the author(s).

ORCID

James Parker  <http://orcid.org/0000-0001-9770-7384>

Data availability statement

The data that support the findings of this study are available from the corresponding author, [James Parker], upon reasonable request.

References

- Aflaki, A., Mirnezhad, M., Ghaffarianhoseini, A., Ghaffarianhoseini, A., Omrany, H., Wang, Z. H., & Akbari, H. (2017). Urban heat island mitigation strategies: A state-of-the-art review on Kuala Lumpur, Singapore and Hong Kong. *Cities*, 62, 131–145. <https://doi.org/10.1016/j.cities.2016.09.003>
- Akbari, H., & Kolokotsa, D. (2016). Three decades of urban heat islands and mitigation technologies research. *Energy & Buildings*, 133, 834–852. <https://doi.org/10.1016/j.enbuild.2016.09.067>
- Aleksandrowicz, O., Vuckovic, M., Kiesel, K., & Mahdavi, A. (2017). Current trends in urban heat island mitigation research: Observations based on a comprehensive research repository. *Urban Climate*, 21, 1–26. <https://doi.org/10.1016/j.uclim.2017.04.002>
- Azevedo, J. A., Chapman, L., & Muller, C. L. (2016). Quantifying the daytime and night-time urban heat island in Birmingham, UK: A comparison of satellite derived land surface temperature and high resolution air temperature observations. *Remote Sensing*, 8(2), 153. <https://doi.org/10.3390/rs8020153>
- Bartasaghi Koc, C., Osmond, P., & Peters, A. (2018). Evaluating the cooling effects of green infrastructure: A systematic review of methods, indicators and data sources. *Solar Energy*, 166, 486–508. <https://doi.org/10.1016/j.solener.2018.03.008>
- Bernard, J., Musy, M., Calmet, I., Bocher, E., & Keravec, P. (2017). Urban heat island temporal and spatial variations: Empirical modeling from geographical and meteorological data. *Building & Environment*, 125, 423–438. <https://doi.org/10.1016/j.buildenv.2017.08.009>
- Blazejczyk, K., Jendritzky, G., Bröde, P., Baranowski, J., Fiala, D., Bulek, G., Havenith, G., Bulek, Y., Epstein, Y., Psikuta, B., & Kampmann, B. (2013). An introduction to the universal thermal climate index (UTCI). *Geographia Polonica*, 86(1), 5–10. <https://doi.org/10.7163/GPol.2013.1>
- Blue Maestro. (2021). *Tempo disc product specification, in, blue maestro*.
- Bowler, D. E., Buyung-Ali, L., Knight, T. M., Pullin, A. S. (2010). Urban greening to cool towns and cities: A systematic review of the empirical evidence. *Landscape and Urban Planning*, 97(3), 147–155. <https://doi.org/10.1016/j.landurbplan.2010.05.006>
- Bröde, P., Fiala, D., Blazejczyk, K., Holmér, I., Jendritzky, G., Kampmann, B., Tinz, B., & Havenith, G. (2012). Deriving the operational procedure for the universal thermal climate index (UTCI). *International Journal of Biometeorology*, 56(3), 481–494. <https://doi.org/10.1007/s00484-011-0454-1>

- Broede, P., Jendritzky, G., Fiala, D., & Havenith, G. (2010). *The universal thermal climate index UTCI in operational use*, in. Loughborough University.
- Chandramathy, I., & Kitchley, J. L. (2018). Study and analysis of efficient green cover types for mitigating the air temperature and urban heat island effect. *International Journal of Global Warming*, 14(2), 238–259. <https://doi.org/10.1504/IJGW.2018.090182>
- Cui, Y., Yan, D., Hong, T., & Ma, J. (2017). Temporal and spatial characteristics of the urban heat island in Beijing and the impact on building design and energy performance. *Energy (Oxford)*, 130, 286–297. <https://doi.org/10.1016/j.energy.2017.04.053>
- Demanuele, C., Mavrogianni, A., Davies, M., Kolokotroni, M., & Rajapaksha, I. (2012). Using localised weather files to assess overheating in naturally ventilated offices within London’s urban heat island. *Building Services Engineering Research & Technology*, 33(4), 351–369. <https://doi.org/10.1177/0143624411416064>
- DiNapoli, C., Messeri, A., Novák, M., Rio, J., Wieczorek, J., Morabito, M., Silva, P., Crisci, A., & Pappenberger, F. (2021). The universal thermal climate index as an operational forecasting tool of human biometeorological conditions in Europe. In E. L. Krüger (Ed.), *Applications of the universal thermal climate index UTCI in biometeorology: Latest developments and case studies* (pp. 193–208). Springer International Publishing.
- Dobrovolný, P., & Krahula, L. (2015). The spatial variability of air temperature and nocturnal urban heat island intensity in the city of Brno, Czech Republic. *Moravian Geographical Reports*, 23(3), 8–16. <https://doi.org/10.1515/mgr-2015-0013>
- Doick, K. J., Peace, A., & Hutchings, T. R. (2014). The role of one large greenspace in mitigating London’s nocturnal urban heat island. *Science of the Total Environment*, 493, 662–671. <https://doi.org/10.1016/j.scitotenv.2014.06.048>
- Emmanuel, R., & Loconsole, A. (2015). Green infrastructure as an adaptation approach to tackling urban overheating in the Glasgow Clyde Valley Region, UK. *Landscape and Urban Planning*, 138, 71–86. <https://doi.org/10.1016/j.landurbplan.2015.02.012>
- Erell, E., Pearlmutter, D., Boneh, D., & Kutiel, P. B. (2014). Effect of high-albedo materials on pedestrian heat stress in urban street canyons. *Urban Climate*, 10, 367–386. <https://doi.org/10.1016/j.uclim.2013.10.005>
- Gaffin, S. R., Rosenzweig, C., Khanbilvardi, R., Parshall, L., Mahani, S., Glickman, H., Goldberg, R., Blake, R., Slosberg, R. B., & Hillel, D. (2008). Variations in New York city’s urban heat island strength over time and space. *Theoretical and Applied Climatology*, 94(1–2), 1–11. <https://doi.org/10.1007/s00704-007-0368-3>
- Giridharan, R., Lau, S. S. Y., & Ganesan, S. (2005). Nocturnal heat island effect in urban residential developments of Hong Kong. *Energy & Buildings*, 37(9), 964–971. <https://doi.org/10.1016/j.enbuild.2004.12.005>
- Grimmond, S. (2007). Urbanization and global environmental change: Local effects of urban warming. *The Geographical Journal*, 173(1), 83–88. https://doi.org/10.1111/j.1475-4959.2007.232_3.x
- Guattari, C., Evangelisti, L., & Balaras, C. A. (2018). On the assessment of urban heat island phenomenon and its effects on building energy performance: A case study of Rome (Italy). *Energy & Buildings*, 158, 605–615. <https://doi.org/10.1016/j.enbuild.2017.10.050>
- Herath, H. M. P. I. K., Halwatura, R. U., & Jayasinghe, G. Y. (2018a). Evaluation of green infrastructure effects on tropical Sri Lankan urban context as an urban heat island adaptation strategy. *Urban Forestry & Urban Greening*, 29, 212–222. <https://doi.org/10.1016/j.ufug.2017.11.013>
- Herath, H. M. P. I. K., Halwatura, R. U., & Jayasinghe, G. Y. (2018b). Modeling a tropical urban context with green walls and green roofs as an urban heat island adaptation strategy, in. *Procedia Engineering*, 212, 691–698. <https://doi.org/10.1016/j.proeng.2018.01.089>
- Hersbach, H., Bell, B., Berrisford, P., Biavati, G., Horányi, A., Muñoz Sabater, J., Nicolas, J., Peubey, C., Radu, R., Rozum, I., Schepers, D., Simmons, A., Soci, C., Dee, D., & Thépaut, J.-N. (2023). *ERA5 hourly data on single levels from 1940 to present*. in: *Copernicus climate change service (C3S) climate data store (CDS)* (ed.), European Centre for Medium-Range Weather Forecasts.
- Huang, J., Kong, F., Yin, H., Middel, A., Liu, H., & Meadows, M. E. (2023). Green roof effects on urban building surface processes and energy budgets. *Energy Conversion and Management*, 287, 117100. <https://doi.org/10.1016/j.enconman.2023.117100>
- Huang, Q., & Lu, Y. (2018). Urban heat island research from 1991 to 2015: A bibliometric analysis. *Theoretical and Applied Climatology*, 131(3–4), 1055–1067. <https://doi.org/10.1007/s00704-016-2025-1>
- Jacobs, C., Singh, T., Gorti, G., Iftikhar, U., Saeed, S., Syed, A., Abbas, F., Ahmad, B., Bhadwal, S., & Siderius, C. (2019). Patterns of outdoor exposure to heat in three South Asian cities. *Science of the Total Environment*, 674, 264–278. <https://doi.org/10.1016/j.scitotenv.2019.04.087>
- Jansson, C., Jansson, P. E., & Gustafsson, D. (2007). Near surface climate in an urban vegetated park and its surroundings. *Theoretical and Applied Climatology*, 89(3–4), 185–193. <https://doi.org/10.1007/s00704-006-0259-z>
- Jenkins, K., Hall, J., Glenis, V., Kilsby, C., McCarthy, M., Goodess, C., Smith, D., Malleon, N., & Birkin, M. (2014). Probabilistic spatial risk assessment of heat impacts and adaptations for London. *Climatic Change*, 124(1), 105–117. <https://doi.org/10.1007/s10584-014-1105-4>
- Kamarianakis, Y., Li, X., Turner, I., B. L., & Brazel, A. J. (2017). On the effects of landscape configuration on summer diurnal temperatures in urban residential areas: Application in Phoenix, AZ. *Frontiers of Earth Science*, 13(3), 1–19. <https://doi.org/10.1007/s11707-017-0678-4>
- Kawashima, S., Ishida, T., Minomura, M., & Miwa, T. (2000). Relations between surface temperature and air temperature on a local scale during winter nights. *Journal of Applied Meteorology*, 39(9), 1570–1579. [https://doi.org/10.1175/1520-0450\(2000\)039<1570:RBSTAA>2.0.CO;2](https://doi.org/10.1175/1520-0450(2000)039<1570:RBSTAA>2.0.CO;2)
- Kolokotroni, M., Ren, X., Davies, M., & Mavrogianni, A. (2012). London’s urban heat island: Impact on current and future energy consumption in office buildings. *Energy & Buildings*, 47, 302–311. <https://doi.org/10.1016/j.enbuild.2011.12.019>
- Konasova, S. (2017). The efficiency of green roofs to mitigate urban heat island effect in Rio De Janeiro. *Advances and Trends in Engineering Sciences and Technologies II - Proceedings of the 2nd International Conference on Engineering Sciences and Technologies, ESAT 2016*, High

- Tatras Mountains, Tatranské Matliare, Slovak Republic, (pp. 465–470).
- Kumar, P., Zavala-Reyes, J. C., Tomson, M., & Kalaiarasan, G. (2022). Understanding the effects of roadside hedges on the horizontal and vertical distributions of air pollutants in street canyons. *Environment International*, 158, 106883. <https://doi.org/10.1016/j.envint.2021.106883>
- Lemke, B. (2010). Excel heat stress calculator. *Health and Environment International Trust*.
- Levermore, G. J., Parkinson, J. B., Laycock, P. J., & Lindley, S. (2015). The urban heat island in manchester 1996–2011. *Building Services Engineering Research & Technology*, 36(3), 343–356. <https://doi.org/10.1177/0143624414549388>
- Levermore, G., & Parkinson, J. (2016). The Manchester urban heat island and adjustments for the chartered institution of building services engineer calculations. *Building Services Engineering Research & Technology*, 37(2), 128–135. <https://doi.org/10.1177/0143624415613951>
- Levermore, G., & Parkinson, J. (2019). The urban heat island of London, an empirical model. *Building Services Engineering Research & Technology*, 40(3), 290–295. <https://doi.org/10.1177/0143624418822878>
- Levermore, G., Parkinson, J., Lee, K., Laycock, P., & Lindley, S. (2018). The increasing trend of the urban heat island intensity. *Urban Climate*, 24, 360–368. <https://doi.org/10.1016/j.uclim.2017.02.004>
- Li, T., Horton, R. M., & Kinney, P. L. (2013). Projections of seasonal patterns in temperature-related deaths for Manhattan. *New York, Nature Climate Change*, 3(8), 717–721. <https://doi.org/10.1038/nclimate1902>
- Lin, J., Wei, K., & Guan, Z. (2024). Exploring the connection between morphological characteristic of built-up areas and surface heat islands based on MSPA. *Urban Climate*, 53, 101764. <https://doi.org/10.1016/j.uclim.2023.101764>
- Lin, P., Lau, S. S. Y., Qin, H., & Gou, Z. (2017). Effects of urban planning indicators on urban heat island: A case study of pocket parks in high-rise high-density environment. *Landscape and Urban Planning*, 168, 48–60. <https://doi.org/10.1016/j.landurbplan.2017.09.024>
- Mahdavi, A., Kiesel, K., & Vuckovic, M. (2016). Methodologies for UHI analysis: Urban heat island phenomenon and related mitigation measures in central Europe. *Counteracting Urban Heat Island Effects in a Global Climate Change Scenario*, 71–91.
- Manes, F., Marando, F., Capotorti, G., Blasi, C., Salvatori, E., Fusaro, L., Ciancarella, L., Mircea, M., Marchetti, M., Chirici, G., & Munafò, M. (2016). Regulating ecosystem services of forests in ten Italian metropolitan cities: Air quality improvement by PM10 and O3 removal. *Ecological Indicators*, 67, 425–440. <https://doi.org/10.1016/j.ecolind.2016.03.009>
- Marando, F., Heris, M. P., Zulian, G., Udías, A., Mentaschi, L., Chrysoulakis, N., Parastatidis, D., & Maes, J. (2022). Urban heat island mitigation by green infrastructure in European functional urban areas. *Sustainable Cities and Society*, 77, 103564. <https://doi.org/10.1016/j.scs.2021.103564>
- Mavrogianni, A., Davies, M., Batty, M., Belcher, S. E., Bohnstengel, S. I., Carruthers, D., Chalabi, Z., Croxford, B., Demanuele, C., Evans, S., Giridharan, R., Hacker, J. N., Hamilton, I., Hogg, C., Hunt, J., Kolokotroni, M., Martin, C., Milner, J. . . . Ye, Z. (2011). The comfort, energy and health implications of London's urban heat island. *Building Services Engineering Research & Technology*, 32(1), 35–52. <https://doi.org/10.1177/0143624410394530>
- Meili, N., Manoli, G., Burlando, P., Carmeliet, J., Chow, W. T. L., Coutts, A. M., Roth, M., Velasco, E., Vivoni, E. R., & Faticchi, S. (2021). Tree effects on urban microclimate: Diurnal, seasonal, and climatic temperature differences explained by separating radiation, evapotranspiration, and roughness effects. *Urban Forestry & Urban Greening*, 58, 126970. <https://doi.org/10.1016/j.ufug.2020.126970>
- Mirzaei, P. A., & Haghighat, F. (2010). Approaches to study urban heat island - abilities and limitations. *Building & Environment*, 45(10), 2192–2201. <https://doi.org/10.1016/j.buildenv.2010.04.001>
- Mohajerani, A., Bakaric, J., & Jeffrey-Bailey, T. (2017). The urban heat island effect, its causes, and mitigation, with reference to the thermal properties of asphalt concrete. *Journal of Environmental Management*, 197, 522–538. <https://doi.org/10.1016/j.jenvman.2017.03.095>
- Ng, E., Chen, L., Wang, Y., & Yuan, C. (2012). A study on the cooling effects of greening in a high-density city: An experience from Hong Kong. *Building & Environment*, 47(1), 256–271. <https://doi.org/10.1016/j.buildenv.2011.07.014>
- Norton, B. A., Coutts, A. M., Livesley, S. J., Harris, R. J., Hunter, A. M., & Williams, N. S. G. (2015). Planning for cooler cities: A framework to prioritise green infrastructure to mitigate high temperatures in urban landscapes. *Landscape and Urban Planning*, 134, 127–138. <https://doi.org/10.1016/j.landurbplan.2014.10.018>
- Oikonomou, E., Davies, M., Mavrogianni, A., Biddulph, P., Wilkinson, P., & Kolokotroni, M. (2012). Modelling the relative importance of the urban heat island and the thermal quality of dwellings for overheating in London. *Building & Environment*, 57, 223–238. <https://doi.org/10.1016/j.buildenv.2012.04.002>
- Oke, T. R. (1976). The distinction between canopy and boundary-layer urban heat islands. *Atmosphere*, 14(4), 268–277. <https://doi.org/10.1080/00046973.1976.9648422>
- Oke, T. R. (1982). The energetic basis of the urban heat island. *Quarterly Journal of the Royal Meteorological Society*, 108(455), 1–24. <https://doi.org/10.1002/qj.49710845502>
- O'Lenick, C. R., Wilhelmi, O. V., Michael, R., Hayden, M. H., Baniassadi, A., Wiedinmyer, C., Monaghan, A. J., Crank, P. J., & Sailor, D. J. (2019). Urban heat and air pollution: A framework for integrating population vulnerability and indoor exposure in health risk analyses. *Science of the Total Environment*, 660, 715–723. <https://doi.org/10.1016/j.scitotenv.2019.01.002>
- Parker, J. (2021). The Leeds urban heat island and its implications for energy use and thermal comfort. *Energy & Buildings*, 235, 110636. <https://doi.org/10.1016/j.enbuild.2020.110636>
- Ramsey, J. D., & Bernard, T. E. (2000). Heat stress. In R. Harris (Ed.), *Patty's industrial hygiene and toxicology* (Vol. 2), (pp. 925–984). John Wiley & Sons.
- Santamouris, M. (2007). Heat island research in Europe: The state of the art. *Advances in Building Energy Research*, 1(1), 123–150. <https://doi.org/10.1080/17512549.2007.9687272>
- Santamouris, M. (2014). Cooling the cities - a review of reflective and green roof mitigation technologies to fight heat island and improve comfort in urban environments. *Solar Energy*, 103, 682–703. <https://doi.org/10.1016/j.solener.2012.07.003>

- Santamouris, M., Gaitani, N., Spanou, A., Saliari, M., Giannopoulou, K., Vasilakopoulou, K., & Kardomateas, T. (2012). Using cool paving materials to improve microclimate of urban areas – design realization and results of the flisvos project. *Building & Environment*, 53, 128–136. <https://doi.org/10.1016/j.buildenv.2012.01.022>
- Sauerbrei, R., Aue, B., Krippes, C., Diehl, E., & Wolters, V. (2017). Bioenergy and biodiversity: Intensified biomass extraction from hedges impairs habitat conditions for birds. *Journal of Environmental Management*, 187, 311–319. <https://doi.org/10.1016/j.jenvman.2016.11.052>
- Skelhorn, C. P., Levermore, G., & Lindley, S. J. (2016). Impacts on cooling energy consumption due to the UHI and vegetation changes in Manchester, UK. *Energy & Buildings*, 122, 150–159. <https://doi.org/10.1016/j.enbuild.2016.01.035>
- Speak, A. F., Rothwell, J. J., Lindley, S. J., & Smith, C. L. (2013). Reduction of the urban cooling effects of an intensive green roof due to vegetation damage. *Urban Climate*, 3, 40–55. <https://doi.org/10.1016/j.uclim.2013.01.001>
- Stewart, I. D. (2011). A systematic review and scientific critique of methodology in modern urban heat island literature. *International Journal of Climatology*, 31(2), 200–217. <https://doi.org/10.1002/joc.2141>
- Sun, C. Y., Lin, Y. J., Sung, W. P., Ou, W. S., & Lu, K. M. (2012). Green roof as a green material of building in mitigating heat island effect in Taipei city, in. *Applied Mechanics & Materials*, 193–194, 368–371. <https://doi.org/10.4028/www.scientific.net/AMM.193-194.368>
- Taha, H. (1997). Urban climates and heat islands: Albedo, evapotranspiration, and anthropogenic heat. *Energy & Buildings*, 25(2), 99–103. [https://doi.org/10.1016/S0378-7788\(96\)00999-1](https://doi.org/10.1016/S0378-7788(96)00999-1)
- Taleghani, M., Marshall, A., Fitton, R., & Swan, W. (2019). Renaturing a microclimate: The impact of greening a neighbourhood on indoor thermal comfort during a heat-wave in Manchester, UK. *Solar Energy*, 182, 245–255. <https://doi.org/10.1016/j.solener.2019.02.062>
- Taleghani, M., Sailor, D. J., Tenpierik, M., & van den Dobbelsteen, A. (2014). Thermal assessment of heat mitigation strategies: The case of Portland State University, Oregon, USA. *Building & Environment*, 73, 138–150. <https://doi.org/10.1016/j.buildenv.2013.12.006>
- Taylor, J., Wilkinson, P., Picetti, R., Symonds, P., Heaviside, C., Macintyre, H. L., Davies, M., Mavrogianni, A., & Hutchinson, E. (2017). Comparison of built environment adaptations to heat exposure and mortality during hot weather, West Midlands region, UK. *Environment International*, 111, 287–294. <https://doi.org/10.1016/j.envint.2017.11.005>
- Tomlinson, C. J., Prieto-Lopez, T., Bassett, R., Chapman, L., Cai, X. M., Thornes, J. E., & Baker, C. J. (2013). Showcasing urban heat island work in Birmingham - measuring, monitoring, modelling and more. *Weather*, 68(2), 44–49. <https://doi.org/10.1002/wea.1998>
- Vaz Monteiro, M., Doick, K. J., Handley, P., & Peace, A. (2016). The impact of greenspace size on the extent of local nocturnal air temperature cooling in London. *Urban Forestry & Urban Greening*, 16, 160–169. <https://doi.org/10.1016/j.ufug.2016.02.008>
- Wang, C., Ren, Z., Dong, Y., Zhang, P., Guo, Y., Wang, W., & Bao, G. (2022). Efficient cooling of cities at global scale using urban green space to mitigate urban heat island effects in different climatic regions. *Urban Forestry & Urban Greening*, 74, 127635. <https://doi.org/10.1016/j.ufug.2022.127635>
- Wang, Y., & Akbari, H. (2016). Analysis of urban heat island phenomenon and mitigation solutions evaluation for Montreal. *Sustainable Cities and Society*, 26, 438–446. <https://doi.org/10.1016/j.scs.2016.04.015>
- Watkins, R., Palmer, J., Kolokotroni, M., & Littlefair, P. (2002). The balance of the annual heating and cooling demand within the London urban heat island. *Building Services Engineering Research & Technology*, 23(4), 207–213. <https://doi.org/10.1191/0143624402bt043oa>
- Wu, J., Zhou, Y., Gao, Y., Fu Joshua, S., Johnson Brent, A., Huang, C., Kim, Y.-M., & Liu, Y. (2014). Estimation and uncertainty analysis of impacts of future heat waves on mortality in the Eastern United States. *Environmental Health Perspectives*, 122(1), 10–16. <https://doi.org/10.1289/ehp.1306670>
- Yamashita, S., & Sekine, K. (1990). Some studies on the earth's surface conditions relating to the urban heat island. *Energy & Buildings*, 15(C), 279–288. [https://doi.org/10.1016/0378-7788\(90\)90140-E](https://doi.org/10.1016/0378-7788(90)90140-E)
- Zhang, J., Hou, Y., Li, G., Van, H., Yang, L., & Yao, F. (2005). The diurnal and seasonal characteristics of urban heat island variation in Beijing city and surrounding areas and impact factors based on remote sensing satellite data. *Science in China Series D: Earth Sciences*, 48(SUPPL.2), 220–229.
- Zhang, P., Imhoff, M. L., Wolfe, R. E., & Bounoua, L. (2010). Characterizing urban heat islands of global settlements using MODIS and nighttime lights products. *Canadian Journal of Remote Sensing*, 36(3), 185–196. <https://doi.org/10.5589/m10-039>
- Zhang, Q., Zhou, D., Xu, D., & Rogora, A. (2022). Correlation between cooling effect of green space and surrounding urban spatial form: Evidence from 36 urban green spaces. *Building & Environment*, 222, 109375. <https://doi.org/10.1016/j.buildenv.2022.109375>
- Zhou, D., Zhao, S., Liu, S., Zhang, L., & Zhu, C. (2014). Surface urban heat island in China's 32 major cities: Spatial patterns and drivers. *Remote Sensing of Environment*, 152, 51–61. <https://doi.org/10.1016/j.rse.2014.05.017>